Republic of Iraq
Ministry of Higher Education
And Scientific Research
University of Anbar
College of Engineering
Mechanical Engineering Department

INVESTIGATIONS OF PHASE CHANGE MATERIALS USED IN SOLAR ENERGY SYSTEMS AS THERMAL ENERGY STORAGE

A Thesis

Submitted to the College of Engineering of University of Anbar in Partial Fulfillment of the Requirements for the Degree of Master of Science in Mechanical Engineering

By

Balqies Abed Abbas Al-fahdawi

(B.Sc. in Mechanical Engineering-2018)

Supervised by

Asst. Prof. Dr. Mustafa B. Al-hadithi

2022 A. D **1443 A. H**

Supervisor's Certification

I certify that this thesis entitled ***"Investigations of Phase Change Materials used in Solar Energy Systems as Thermal Energy Storage"*** was prepared by ***" Balqies Abed Abbas"*** under my supervision at College of Engineering / University of Anbar in partial fulfillment of the requirements for the degree of **Master of Science in Mechanical Engineering**.

Signature:
Name: Asst. Prof. Dr. Mustafa B. Al-hadithi
Date: / / 2022

In view of the available recommendation, I forward this thesis for debate by the examining committee.

Signature:
Name: Asst. prof. Dr. Saad M. Jalil
Head of the Mechanical Engineering Department
Date: / / 2022

Linguist Certification

This is to certify that I have read the thesis titled ***“Investigations of Phase Change Materials used in Solar Energy Systems as Thermal Energy Storage”*** and corrected any grammatical mistake I found. The thesis is therefore qualified for debate as far as language is concerned.

Signature

Name :

Date: / / 2022

Committee Certification

We certify, as an Examining Committee, that we have read this thesis entitled ***"Investigations of Phase Change Materials used in Solar Energy Systems as Thermal Energy Storage"*** and examined the student *" **Balqies Abed Abbas**"* in its content and what related to it, and found it adequate for the standard of a thesis for the degree of **Master of Science** in **Mechanical Engineering.**

Prof. Dr.
(Chairman)
/ / 2022

Asst. Prof. Dr.
(Member)
/ / 2022

Asst. Prof. Dr.
(Member)
/ / 2022

Prof. Dr.
(Supervisor and Member)
/ / 2022

Approved by the College of Engineering / AL- Anbar University

Asst. Prof. Dr. Ameer Abdulrahman Hilal
Dean of the College of Engineering

DECLARATION

I hereby declare that this thesis, submitted to Anbar university as a requirement for the master degree has not been submitted as an exercise for a similar degree at any other university. I also support this work that is qualified here is entirely my own except for excerpts and summaries whose sources are congruently cited in the references.

Balqies Abed Abbas

2022

ABSTRACT

This study address to numerically investigate the performance and behavior of the phase change material (PCM)during melting and solidification process inside the annulus between two concentric pipes. Local paraffin wax has selected as PCM, which has a melting temperature of 334K. Water is chosen as the heat transfer fluid flows through the inner pipe (hot water for charging and cold water for discharging). The thermal conditions of the outer pipe was selected to be insulated (adiabatic) and the inner pipe was kept at constant temperature (isothermal). Finite volume method (FVM) is used to solve the governing equations of transient fully developed laminar flow. The fluid flow in the mushy zone was accounted for using the Darcy drag source term in momentum equation, and the liquid percentage in each cell was updated using the enthalpy-porosity method. The outcomes of the simulation are represented as contours of average temperature and liquid fraction distribution in the flow domain. The simulation findings indicate that convective heat transmission has considerable impact on the melting of the upper zone of the (PCM) but has less impact on the melting of the lower zone. It is obvious that the melting process ends up with a relatively short period of time in the top region, followed by the middle region, and finally the bottom region of the annulus. During the solidification process, natural convection plays a role only during the early periods of solidification and then thermal conduction remains the dominant heat transfer mode for the entire process. The predicted result shows the capturing phenomenon: primary heat conduction in all regions and then heat convection and conduction become dominant in the top and bottom regions, respectively. The maximum and minimum temperature changes near the outer pipe surface during the 16 hours are 56.25 % and 42.5 %, respectively.

LIST OF CONTENTS

Contents	Page

Abstract	I
List of Contents	II
List of Tables	V
List of Figures	VI
List of Symbols	VII
List of Abbreviations	IX
Chapter One: Introduction	**1**
1.1 Background	1
1.2 Thermal Energy Storage	3
1.3 Phase Change Materials	5
1.3.1 Organic Materials	6
1.3.2 Inorganic Materials	7
1.3.3 Eutectic Materials	7
1.4 Problem Statement	8
1.5 Aim and Objectives of Current study	9
1.6 Thesis Outlines	10
Chapter Two: Literature Review	**11**
2.1 Introduction	11
2.2 Experimental Investigations	11

2.3 Numerical Investigations	14
2.4 Experimental and Numerical Investigations	23
2.5 Summary	28
Chapter Three: Mathematical Model and Numerical Solution	**45**
3.1 Introduction	45
3.2 Research Approach	45
3.3 Physical Model	48
3.4 Thermophysical Properties and Assumptions	49
3.5 Governing Equations	50
3.6 Boundary and Initial Conditions	53
3.7 Numerical Solution and Mesh Dependency	54
3.8 Computational Grid	56
3.9 CFD Modeling and Simulation	57
Chapter Four: Results and Discussion	**58**
4.1 Overview	58
4.2 Validation Tests	58
4.3 Solidification Process	60
4.4 Melting Process	68
Chapter Five: Conclusion and Recommendations	**77**
5.1 Conclusion	77
5.2 Recommendations and Future work	79

References **80**

LIST OF TABLES

Table	Title	Page No.
2.1	Summary of the experimental studies.	29
2.2	Summary of the numerical studies.	32
2.3	Summary of the experimental and numerical studies.	40
3.1	Dimensions and materials of the concentric pipes.	49
3.2	Thermophysical properties of used materials [32].	49
3.3	Thermo-physical Properties of PCM in Temperature Range 300K < T < 350K.	50
3.4	Mesh dependency in the present study for PCM average temperature after 3 hours of solidification process.	54
3.5	Mesh dependency in the present study for PCM liquid fraction after 3 hours of solidification process.	54
4.1	Temperature changes near the outer pipe surface during 16 hrs.	66
4.2	Liquid fraction changes in the annulus during 16 hrs. according to $\dot{R}R$ value.	66

LIST OF FIGURES

Figure	Title	Page No.
1.1	PCM thermal storage arrangement for a domestic solar water heating system [6].	3
1.2	Classification of thermal energy storage [7].	5
1.3	The melting and solidification processes of phase change materials [9].	6
1.4	Classification of PCM [10].	8
1.5	Double pipe heat exchanger.	9
3.1	Flow chart of the numerical study	47
3.2	Schematic of the concentric annulus pipes: (a) 3D view ,(b) Cross section view.	48
3.3	Computational domain with boundary conditions: (a) Solidification process, (b) Melting process.	53
3.4	Mesh dependency tests for PCM average temperature.	55
3.5	Mesh dependency tests for PCM liquid fraction.	55
3.6	Mesh generation for the physical domain.	57
4.1	Comparison of temperature profile vs. previous studies Al-Abidi et al[20] and Jasim et al[28] .	59
4.2	Comparison of the temperature profile with previous studies by Al-Abidi et al[20] and Al-Mudhafar et al[29].	60
4.3	Contours of PCM transient temperature during discharging process.	62
4.4	Contours of the PCM transient liquid fraction during discharging process.	63
4.5	Temperature with dimensionless radius for different times and locations in the annulus:(a)Line5,(b)Line 4, (c) Line 3, (d) Line 2,(e) Line1.	65
4.6	Liquid fraction with dimensionless radius for differen times and locations in the annulus: (a)Line5,(b)Line4, (c)Line3,(d)Line2,(e)Line1.	67
4.7	History of PCM average temperature over different line's locations during melting process.	69
4.8	History of PCM liquid fraction over different lines locations during melting process.	70

4.9	Contours of the PCM transient temperature during melting process.	72
4.10	Contours of the PCM transient liquid fraction during melting process**.**	74
4.11	History of local PCM temperature over different line' locations.	75
4.12	History of local PCM liquid fraction over different lines locations.	76

LIST OF SYMBOLES

Nomenclatures

Symbols	**Description**	**Unit**
A	Mushy zone constant	kg/$m^3.s$
a_m	Fraction melted	/
a_r	Fraction reacted	/
C_p	Specific heat	J/kg.K
F	Liquid fraction	/
G	Gravitational acceleration	m/s^2
H	Sensible enthalpy	J/kg
H	Total enthalpy	J/kg
K	Thermal conductivity	W/m.K
L	Latent heat	J/kg
M	Mass of heat storage medium	Kg
Q	Quantity of heat stores	J
RR	Dimensionless annulus radius	/
P	Pressure	Pa
S	Source term	/

T	Time	S
T	Temperature	K
V	Velocity	m/s
ΔH	Latent enthalpy	J/kg
Δh_m	Heat of fusion per unit mass	J/kg
Δh_r	Endothermic heat of reaction	/

Greek letters

ρ	Density($kg/\ m^3$)
μ	Dynamic viscosity ($kg/m\ .\ s$)
ε	Numerical constant.
β	Volume expantion covesiont ($1/K$)

Subscripts

Mush	Mushy zone
Ref	Reference
Solidus	Solid phase
Liquidus	Liquid phase
i	Initial state
m	Melting

LIST OF ABBREVIATIONS

PCM	Phase Change Materials
CFD	Computational Fluid Dynamics
TES	Thermal Energy Storage
LHTES	Latent Heat Thermal Energy Storage
FVM	Finite Volume Method
HTF	Heat Transfer Fluid
LHS	Latent Heat Storage
GIT	Grid Independence Test

CHAPTER ONE

Introduction

1.1 Background

Thermal energy storage (TES) plays significant role in the energy conservation and the development of renewable resources. This type of storage can help resolve the mismatch between the supply energy and the demand as well as boost the dependability of energy production systems [1]. Among different types of thermal energy storage, latent heat thermal energy storage (LHTES) devices have attracted considerable attention worldwide due to their large potential saving of energy and their ability to provide or absorb a relatively large amount of thermal energy [2]. More recently, the thermal storage technique based on the use of phase change materials (PCM) as a storage medium has proved the most effective due to its high storage density and small temperature variation during the processes solid-liquid phase change. These specifications have made PCM promising for many engineering applications, such as solar heaters, cooling/heating systems, solar cookers, drying technology, building air-conditioners, electronic devices cooling, preservation containers of pharmaceutical products and lots of other applications [3].

Among different LHTES systems for heating and cooling applications, double pipe heat exchange are the most common systems due to their simplicity and ease of manufacture. The LHTES device consists primarily of three major components: (a) phase change material, (b) container appropriate for storing PCM, and (c) conductive heat transfer surface or surfaces for transferring heat between the heat source and the PCM, as well as from the PCM to the heat sink [4]. The main criterion for the selection of a PCM for a particular application is the melting temperature or the phase change temperature range of the PCM. Furthermore, with regard to latent heat applications with PCMs, the applications can be categorized into two categories: (i) protection or thermal inertia, and (ii) thermal energy storage. The thermal conductivity of the PCM is one of the major differences between these two sections. In the subject of thermal protection, low thermal conductivity is desirable. On the other hand, the low thermal conductivity values of PCMs make them undesirable for thermal storage systems. The evolution of LHTES systems faces great challenges due to low thermal conductivity of phase change materials, which leads to low heat transfer rate during melting and solidification processes. Furthermore, paraffin wax is used as the most common phase change material for thermal storage applications because it has a large latent heat and low cost besides being stable, non-toxic and non-corrosive [5].

Recently, there is a growing demand for low-cost, efficient, and sustainable energy production without harming the environment. Solar energy has globally considered as an important renewable energy source. However, solar water heaters are one of the most utilized technologies for converting solar energy into thermal energy [6]. Solar water heaters rely heavily on efficient thermal energy storage. In this context, phase change material based latent heat energy storage systems have emerged as a promising option to effectively store thermal energy for solar water heater applications, as illustrated in Figure 1.1. Moreover, understanding the fundamentals of phase change heat transfer processes that occur during the melting and solidification of PCM is crucial for the development of more practical and efficient thermal energy storage systems.

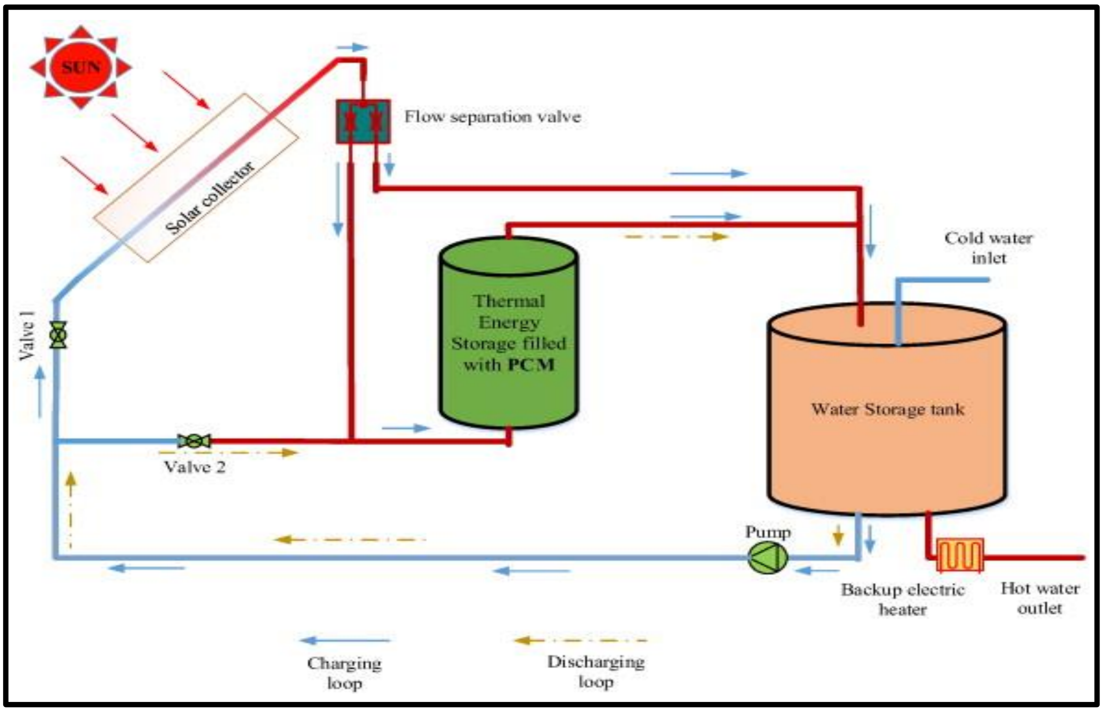

Figure 1.1: PCM thermal storage arrangement for a domestic solar water heating system [6].

1.2 Thermal Energy Storage (TES)

Thermal energy storage is a technology that stocks thermal energy by heating or cooling a storage medium so that the stored energy can be used at a later time for heating and cooling applications and power generation. There are three common ways to store thermal energy: sensible heat, latent heat and thermo-chemical energy [7]. The classification of thermal energy storage is given in Figure 1.2. In sensible heat, energy is stored/released by raising/reducing the temperature of a storage material without changing the phase. The amount of energy stored depends upon the amount of the storage material, the specific heat of the medium, and the difference between the change in temperature at the initial and final stage, as illustrated in the equation (1.1).

$$Q = m \int_{T_i}^{T_f} C_P \, dT = m \, C_p \, (T_f - T_i) \tag{1.1}$$

In latent heat storage systems, the operation of storing and retrieving thermal energy is based on the latent heat of fusion, where the storage medium undergoes a phase transformation. The heat stored during the material's phase change process is referred to as latent heat. The chemical bonds of the PCM material break up when the source temperature rises, resulting in the transition from one phase to another [8]. The material of phase transformation can be solid-solid, solid-liquid, or liquid-gas. Unlike sensible heat, latent heat storage is attractive in that it stores a greater amount of energy at a constant temperature during phase conversion. There are two different types of latent thermal energy: the latent heat of fusion and the latent heat of vaporization. The latent heat of fusion refers to the energy that is absorbed or released during the melting/solidification process. Latent heat is unique in that it is heat that is absorbed into a material without the material itself increasing in temperature. Furthermore, is also important to distinguish it from the other type of latent heat, the latent heat of vaporization, which describes the transition from a liquid to a gas phase. The storage capacity of a latent heat system is given by:

$$Q = m\left[\int_{T_i}^{T_m} C_{p-Solid}\, dT + a_m \Delta h_m + \int_{T_m}^{T_f} C_{p-Liquid}\, dT\right]$$

$$= m\left[C_{p-solid}(T_m - T_i) + a_m \Delta h_m + C_{p-liquid}(T_f - T_m)\right] \qquad (1.2)$$

In thermo-chemical energy storage, heat is absorbed or released through a completely reversible chemical reaction when the molecular bonds are reformed and broken during an endothermic or exothermic reaction. Due to the high cost of such systems, their applications are very limited. Thermal storage relies on the amount of storage material, endothermic heat of reaction, and the extent of conversion given by Equation 1.3.

$$Q = m\, a_r \Delta h_r \qquad (1.3)$$

Amongst above thermal heat storage techniques, latent heat thermal energy storage is especially attractive due to its ability to provide high energy storage density and its characteristics of storing heat at a constant temperature corresponding to the phase transition temperature of PCM. In addition, solid-liquid transitions have proven to be effective in thermal energy storage systems.

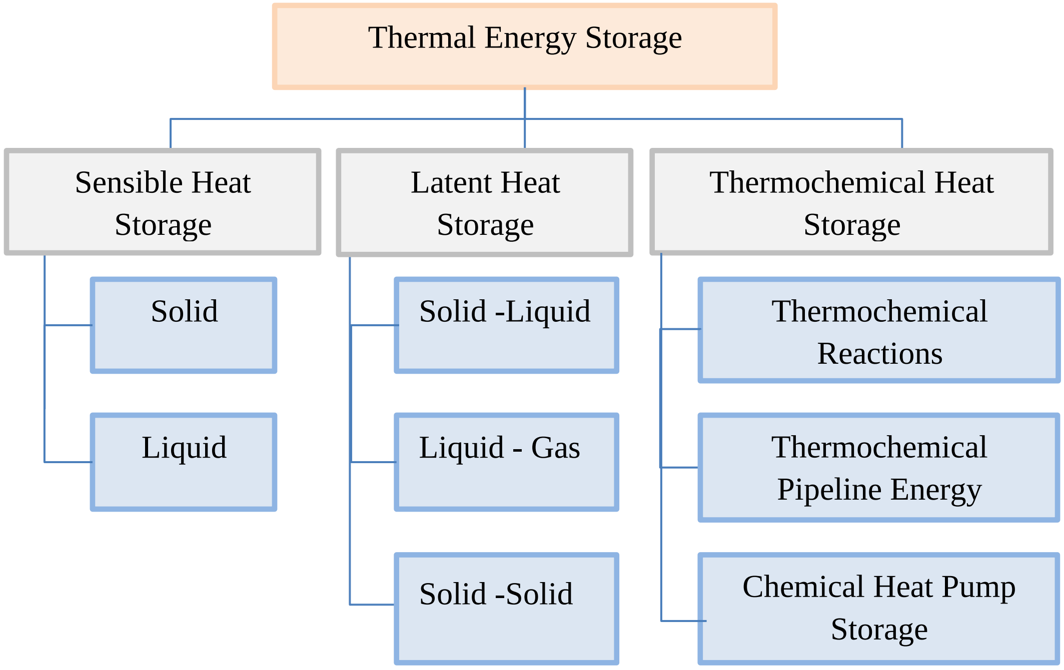

Figure 1.2: Classification of thermal energy storage [7].

1.3 Phase Change Materials (PCM)

Phase change materials (PCMs) are materials that undergo the solid-liquid phase transformation. It is more commonly known as the melting-solidification cycle, at a temperature within the operating range of a selected thermal application. As a material changes phase from a solid to a liquid, it absorbs energy from its surroundings while remaining at a constant or nearly constant temperature. The energy that is absorbed by the material acts to increase the energy of the constituent atoms or molecules, increasing their vibrational state. At the melt temperature, the atomic bonds loosen and the material transitions from a solid to a liquid. Solidification is a reverse of this process, during which the material transfers energy to its surroundings and the molecules lose energy and order themselves into their solid phase [9]. This can be seen in Figure 1.3.

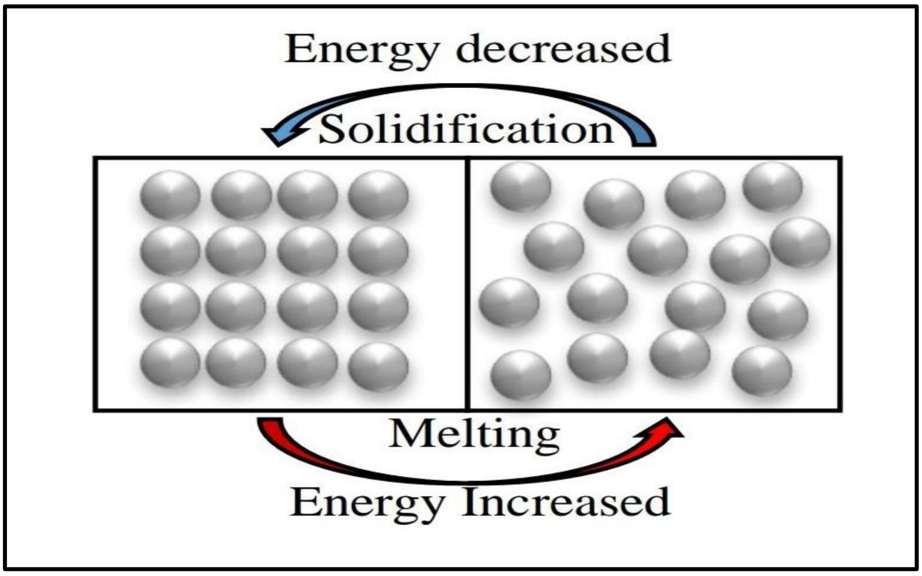

Figure 1.3: The melting and solidification processes of phase change materials [9].

Although there are many different types of PCM, the great majority of them fall into one of three main categories [10]: organics, inorganics, or eutectic. The classification of PCM is illustrated in Figure 1.4. However, the melting point, thermal energy storage density, and thermal conductivity of organic, inorganic, and eutectic phase change materials are the fundamental selection criteria for a wide range of thermal energy storage applications [11]. Moreover, the following section offers a glimpse into each of the major classifications of PCM in further depth.

1.3.1 Organic Materials

Organic PCMs can melt and solidify several times without phase separation, and they crystallize with little or no super cooling due to the depreciation of their latent melting heat [12]. The following are the two major groups:

(1) Paraffin waxes are primarily composed of the straight-chain n-alkenes CH_3–(CH_2)–CH_3.The (CH_3) chain crystallization releases a lot of latent heat. With chain length, both the melting point and the latent heat of fusion rise. Due to cost concerns, only technical grade paraffins may be utilized as PCMs in latent heat storage systems. Paraffin is safe, dependable, predictable, less expensive, non-corrosive, and has a wide temperature range (5–80 °C) [8].

(2) non-paraffin organic PCM are the most common type of PCM, having a wide range of characteristics. A number of esters, fatty acids, alcohols, and glycols that can be used to store energy have been discovered. High heat of fusion, inflammability, low thermal conductivity, low flash points, and instability at high temperatures are all characteristics of these organic materials [13].

1.3.2 Inorganic Materials

Inorganic PCMs are employed in high-temperature solar applications, and one of the most commonly mentioned issues is their upkeep. They freeze at lower temperatures and are difficult to handle at higher temperatures [12].

1.3.3 Eutectic Materials

Eutectic materials are made up of two or more low melting materials with similar (congruent) melting and freezing temperatures; eutectics almost never segregate during melting and freezing and have high thermal conductivities and densities .The melting point of the resulting eutectic mixture can be adjusted by changing the weight proportion of each constituent [12].

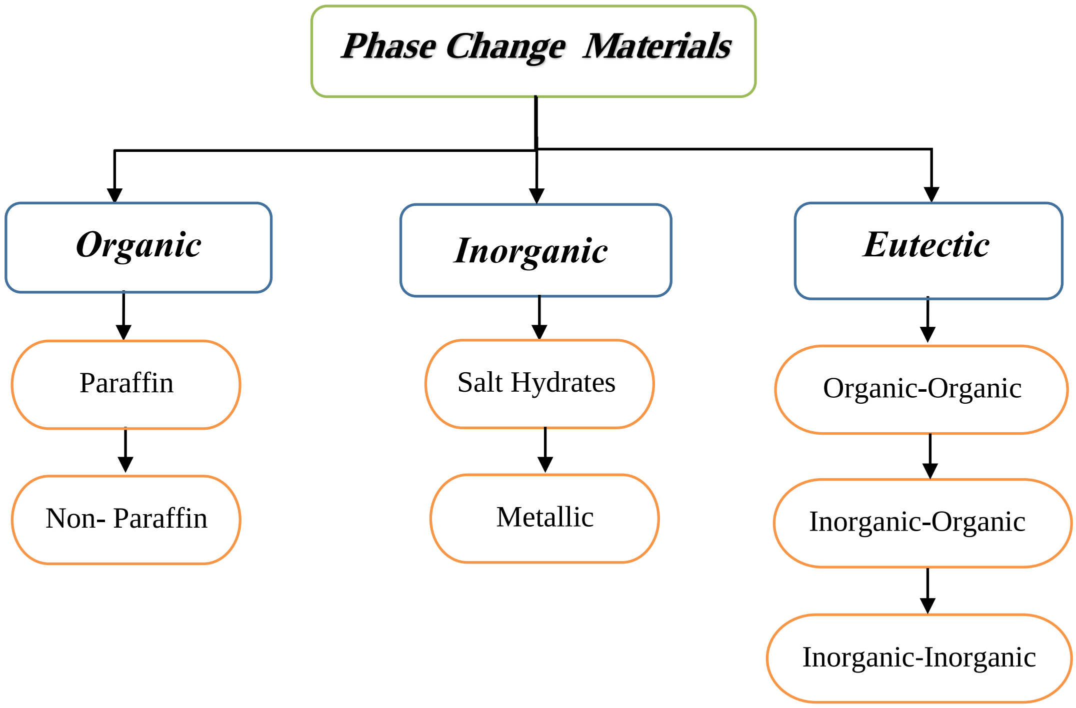

Figure 1.4: Classification of PCM [10].

1.4 Problem Statement

Due to rising energy demands and limited resources, interest in designing energy storage systems for heating and cooling applications has increased in many homes and industries establishments. One of the most promising solutions to this problem is latent heat storage (LHS). Phase change materials are well-established as latent heat storage materials due to their huge energy capacity, moderate temperature variation, chemical stabilities, and low vapour pressure at operating temperature. Several recent studies regarding thermal energy storage systems (particularly their latent form) have optimized the amount of exchanged energy and improved their thermal conductivity. However, there are a few studies that include the performance of PCM, in which the thermal behavior of local paraffin wax has not been widely studied by numerical method due to complexity presence of three phases, such as solid, liquid, and mushy zones, the numerical solution of the melting and solidification of a PCM inside a domain is extremely complicated. It is a challenge to adopt the enthalpy-porosity formulation to track the mushy region at every time instant, particularly in the presence of natural convection. There seems to be no numerical work reported in the literature which has modeled the melting and solidification of a local paraffin wax embedded inside a horizontal concentric annulus. Enthalpy-porosity technique is applied to solve the governing equations in which the natural convection heat transfer is also considered by using ANSYS FLUENT 2020 R2. Simulation results are presented in the forms of liquid fraction, average temperature and their contours. The findings will be useful in many engineering applications, particularly thermal storage applications in heat exchangers. Measures to examine the heat storage capability of the system will then be advantageous to the overall energy savings.

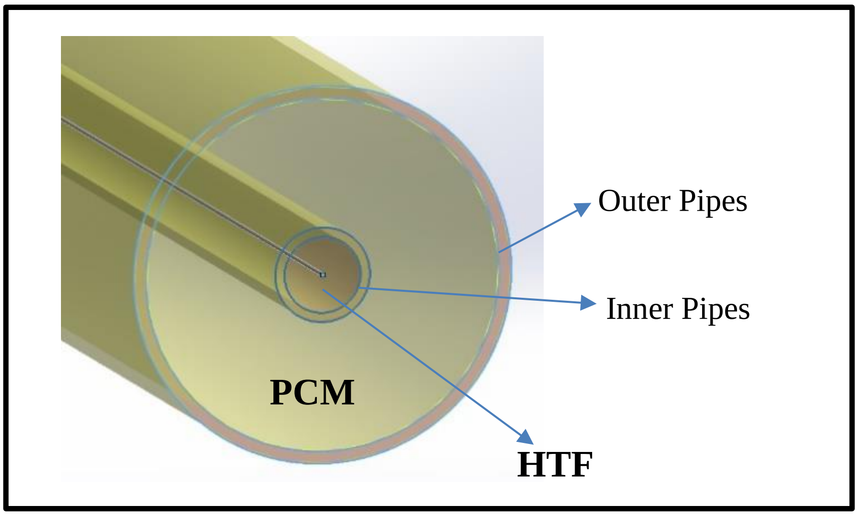

Figure 1.5: Double pipe heat exchanger.

1.5 Aim and Objectives of Current study

The main aim of this study is to investigate numerically the performance of solidification and melting phenomena of local paraffin wax in a concentric annulus pipe. The primary objectives of this study are itemized as follows:

1) To evaluate and analyze of PCM charging and discharging processes in the annulus geometry of a double-pipe heat exchanger.

2) Investigate the history of the thermal behavior of PCM during the solidification and melting processes.

1.6 Thesis Outlines

This dissertation consists of five chapters, and it is briefly offered as follows:

- **Chapter One:** explains the general background, thermal energy storage systems, types of phase change materials, problem statement and the objectives of the current study.
- **Chapter Two:** displays the literature review of numerical and experimental investigations for phase change materials used in thermal energy storage systems and different geometries of the storage systems.
- **Chapter Three:** deals with the mathematical formulations used in the present study. The physical model descriptions, the governing equations, the boundary conditions, and the thermo-physical properties of the PCM are presented. It also explains the numerical procedures used in the present study. The mesh dependency, the computational grid, and CFD modeling and simulation are all covered in this chapter.
- **Chapter Four:** presents the numerical results obtained in the current study. The initial part of this chapter focuses on the validation of the present CFD code. The analysis and discussion of the results of the solidification and melting processes of PCM are described in this chapter.

Chapter Five: defines the key conclusions that have been obtained from the present study and some suggested recommendations for future work.

CAPTER TWO

Literature Review

2.1 Introduction

This chapter displays the previous studies concerned with phase change materials and heat transfer characteristics during the melting and solidification processes of latent heat thermal energy storage (LHTES) systems. The first section reviews the experimental studies that illustrate heat transfer enhancement techniques used in thermal energy storage systems. The second section displays the numerical studies which show the effect of using numerical simulation techniques to predict the thermal behavior of a PCM and optimize the energy storage system configuration. The third section presents the experimental and numerical studies which explain the effect of the operating conditions and changed geometrical parameters on the thermal performance of shell-and-tube LHTES units.

2.2 Experimental Investigations

Akgün et al. [14] studied experimentally the thermal performance of the PCM in a concentric shell and tube system as a vertical heat exchanger during charging and solidification operations. The shell space is filled with paraffin wax as a phase change material (PCM), while water is passed through the inner tube as a heat transfer fluid. The study focused on the enhanced probability of heat transfer by tilting the outer surface of the storage system at an angle of 5 degrees. The tests were performed with varying HTF inlet temperatures of 60, 65, 70, and 75 °C and mass flow rates of 4, 6, and 8 kg/min for both processes. It was found that the total charging time for the above-inclined angle would be reduced by approximately 30%. In addition, the charging time is reduced as the HTF's inlet temperature rises and the mass flow rate decreases.

Rathod and Banerjee [15] presented an experimental study to evaluate the thermal behavior of PCM with melting points of 58 °C and 60 °C as well as the influence of HTF inlet temperature and mass flow rate on the thermal performance of a shell-and-tube heat exchanger. The shell is filled with paraffin wax as a PCM while water as HTF runs through the inner tube. They observed that the melting time of PCM increases as the mass flow rate and inlet temperature of water decrease. The results indicate that the temperature of the inlet water has a significant influence on the improved performance of the PCM storage unit. In addition, the mass flow rate was found to have an insignificant impact on the overall time of charge and discharge. It was found that convection and conduction were the controlling mechanisms for the charging and discharging operations, respectively.

Jesumathy et al. [16] conducted an experimental investigation to study the charging and discharging characteristics of a PCM (paraffin wax) in a double-pipe heat exchanger where the PCM was embedded in the horizontal annulus gap. The influence of the different mass flow rates of the HTF (hot water for melting and cold water for solidification) and the inlet temperature on the thermal performance of the PCM were presented. The authors observed from their experimental results that convection and conduction were controlling mechanisms for the charging and discharging operations, respectively. It was also discovered that raising the inlet HTF temperature to 2 °C increased the heat transfer rate during the charging and discharging processes by 25% and 11%, respectively. Therefore, when the HTF's initial temperature was increased from 70 to 74 degrees Celsius, the total melting time decreased by 31%.

Shen et al. [17] studied experimentally the melting and solidification characteristics of a PCM (paraffin wax RT-60) in a multi-tube LHTES unit where the PCM was embedded in the vertical annulus gap. Their heat storage container consisted of five copper tubes with heat transfer fluid (water) flowing inside the tubes. The goal of adding more pipes was to improve the LHTES unit's efficiency. The thermocouples were positioned in four areas of the unit, with different angular and radial directions, to record the temperature over time for PCM melting and solidification procedures. The results showed that convection in the melting process was a key factor affecting the heat exchanger's performance. At the lowest position, the PCM will solidify quickly due to conduction heat transmission. The quantity and location of tubes in the LHTES units increased the effectiveness of heat transfer in each melting and solidification phase.

Kousha et al. [18] performed an experimental study to evaluate the effect of the number of tubes and HTF inlet temperature on the amount of stored and recovered energy during the melting and solidification operations. The heat storage container was a shell and multi-tube heat exchanger where the heat transfer fluid (water) flowed through the inner tubes (made of copper, with an outer diameter of 12.7, 8.98, 7.33 and 6.35 mm respectively), while the PCM (paraffin wax RT-35) filled the annulus gap of the exchanger (made of Plexiglas, with an inner diameter of 70 mm and a length of 400mm). To reduce heat losses, the shell's outer surface was insulated with a 10mm thick Flex elastomeric. Four different numbers of tubes were selected: one, two, three and four. The findings show that increasing the number of tubes increases the heat transmission area between HTF and PCM, resulting in improved melting and solidification operations. Furthermore, it was found that compared to one tube heat exchanger, the four tubes heat exchanger greatly increases the thermal performance of PCM. It was observed that by increasing the HTF inlet temperature the stored energy increased. Additionally, when the inlet temperature of HTF was at 80 °C, the charge time was reduced by 43%, and when the inlet temperature of HTF was at 10 °C, the discharge time was reduced by 50%.

- <u>Table (2.1) shows a summary of the experimental studies.</u>

2.3 Numerical Investigations

Wang et al. [19] presented a numerical investigation to study the influences of the mass flow rate of HTF and temperature variation between the inlet of water and fusion point of PCM on the melting and solidification behaviors in axis-symmetric of shell and tube latent heat thermal energy storage system. The n-octadecane filled the shell as PCM while the water flowed through the tube as HTF. The governing equations were discretized by using the finite difference method carry out in FORTRAN software. It is observed that the water inlet temperature displayed higher impact on the total time to complete melting and solidification operations. Also, the increase in the water entry temperature leads to increase the storage of heat as the non-linear shape. Moreover, the water flow rate has a minor impact on the quantity of energy stored, but it has a significant impact on charging and discharging time periods.

Al-Abidi et al. [20] conducted a numerical analysis to improve heat transfer by using internal and external fins for PCM during charging operation in a triplex tube storage system. Water was selected as the (HTF) that circulated through the outer and inner tubes, whereas (PCM) was filled in the middle tube. All tubes are composed of copper to provide efficient thermal conductivity and to facilitate heat transmission between the (HTF) and the (PCM). The inner, middle, and outer tubes have a radius of 25 4 mm, 75 mm, and 100 mm, respectively. Also, the inner and outer tubes have a thickness of 1.2 mm and 2 mm, respectively. The simulation was carried out with the ANSYS Fluent program, which uses the enthalpy-porosity approach and finite volume methods. The effects of the number, length and thickness of fins were presented. Their findings showed that as the number and length of fins increased, the time it took for PCM to melt decreased. It means that the length and number of fins have significantly impacted on the heat transfer enhancement of the storage system. Furthermore, the thickness of the fins had minimal impact on the charging cycle. It is found that the different shapes of storage systems with fins have an effect on the heat transfer enhancement compared with those without fins.

Seddegh et al. [21] conducted a numerical investigation of heat transfer enhancement and the performance evaluation in the axis-symmetric for vertical cylindrical LHTES unit. The storage container consists of shell and tube type where the heat transfer fluid (water) flows inside the tube while the paraffin wax at melting temperature 331 K is considered as a PCM filled in an annular space. Effects of the two different models involved utilizing one a pure conduction model and the other a combined conduction-convection model were studied and compared with declared experimental data for charging and discharging phenomena. The unsteady energy and Navier-Stokes equations were solved using the enthalpy method implemented in Fluent ANSYS 15 software. It was concluded that there is a good match between numerical forecasts and experimental data from prior studies. They found that at the charging cycle, the free convection is the major mode of heat transport in the paraffin wax. Moreover, the thermal conduction controlling the discharging cycle. It was observed that the combined model displayed higher heat transfer enhancement for the phase change material than that of the pure conduction.

Seddegh et al. [22] executed a numerical investigation to study effect of horizontal and vertical shell and tube configurations to performance evaluate for LHTES system by utilizing natural convective and conductive heat transfer models. The paraffin wax (RT 50) filled the shell was used as a PCM while the water passed through the inner tube as an HTF. The influence of the entry temperature of water, mass flow rate, heat fraction and total phase transition time for both melting and solidification on the charging and discharging operations behaviors were presented. The governing equations of momentum, continuity and energy for laminar flow were solved numerically by using the enthalpy method implemented in ANSYS 15 software. The predictions of the numerical results were compared with the experimental data obtained from previous researchers. Results showed that the conduction controlled the heat transfer in the both horizontal and vertical configurations during the solidification cycle. They illustrated that the active melting of paraffin was found at the top part better than was found at the bottom part in the horizontal configuration while the melting was equal in the vertical configuration. Furthermore, they observed that the inlet water temperature has maximum impact on the charging cycle for horizontal/vertical configurations compared with that of the mass flow rate which has minimum impact on the charging and discharging cycles for both configurations.

Esapour et al. [23] conducted a numerical investigation on the heat transfer enhancement from the phase change material using multi-tube heat exchangers. The paraffin wax RT 35 is chosen as a PCM filling the shell side while the heat transfer fluid (water) flows through inside tubes. They presented the effects of the mass flow rate and inlet temperature of water during melting operation. Additionally, different numbers of inner tubes: double, triple, and quadruple tubes were presented and compared with the single tube heat exchanger. The governing equations were solved by using the enthalpy porosity method .They found that the highest melting rate occurred when increasing the number of tubes to quadruple tubes which leads to a decrease in melting time up to 29 % compared with the single tube .The numerical results showed that the melt time of paraffin wax decreased with increasing entry temperature of water .whereas, there was doesn't achieved any effect when increasing flow rate of heat transfer fluid on the paraffin melting operation.

Mousavi Ajarostaghi et al. [24] executed a numerical investigation to study the influence of different geometries shapes during the PCM melting cycle to enhance the heat transfer and evaluate performance of latent heat thermal energy storage systems .Their type of thermal storage system was consisted of a shell and tube heat exchanger which water flow through the tube whereas the shell was filled with the PCM at melting temperature 36 ℃. Five types of geometry of channels were selected : circular, rectangular, elliptical, square and diamond shape. The numerical simulation was performed for all shapes studied by using ANSYS FLUENT 6.3 software. The results indicated that free convection quickened thermal energy transport in the charging operation in the upper part but weakened in the lower part. Moreover, thermal conduction at the melt phase was dominated for all-parts. It is found that the vertical rectangular shape reduces melting time up to 75% compared with the circular shape. However, the horizontal rectangular showed the lowest melt specifications compared with other shapes.

Han et al. [25] studied the 2D unsteady laminar melting process in a concentric horizontal/vertical annulus of shell and tube heat exchanger using a finite volume method. Specifically, they modeled two geometrical arrangements. In one case, they considered a pipe model in which the annulus is filled with PCM while HTF flows through the inner tube and in the second case, they considered a cylinder model in which the inner tube is filled with PCM while HTF flows through the annulus. A comparison of horizontal and vertical models with different HTF inlets and evaluation of the effect of natural convection on the charging cycle were present. They found that the PCM melting rate in the horizontal cylinder model was improved by the effect of natural convection more than in the horizontal pipe model. They also reported that the time it takes to finish the melting process has been lowered by 23.5 percent. The results show that the vertical pipe model with an HTF input at the bottom had the maximum PCM melting rate, in contrast to the horizontal and vertical cylinder models where the HTF inlet at the bottom is nearly the same.

Elmeriah et al. [26] presented a numerical study on the heat transfer enhancement between heat transfer fluid and phase change material in the LHTES system using forced convection and conduction. The system is a shell and tube heat exchanger where the water as HTF flows inside the tube whereas the paraffin wax RT 60 as a PCM fills the shell side. The parameters studied were Reynolds number, tube length and shell diameter during charging and discharging operations. Governing equations of two-dimensional models were solved using the enthalpy method implemented in ANSYS Fluent 17 software. They observed that there is a good match between numerical forecasts and experimental data from prior studies. They results showed that Reynolds number have a significant effect on the time and rate of the changing and discharging operations. Also, it was found that the shell diameter and tube length are the most effective parameters which improvement of the storage system performances and have major effect on the exit temperature of water as well as the time of the melting and solidification processes.

Begum et al. [27] carried out a numerical investigation to study the influence of hexagonal shell which fills with paraffin wax as PCM and different shapes tubes models with water flows inside as HTF on the latent heat thermal energy storage system performance during charging cycle at melting temperature 59.9 °C. The shape of tubes that studied here was a circular and vertical and horizontal elliptical. The governing equations were solved numerically by using the finite difference method (FDM). They presented the effects of various inlet temperature and mass flow rate of the heat transfer fluid. Their results indicated that the natural convection affects the melting of the wax in the upper part of the test system more than the wax in the lower part of the test system because of the buoyancy force. In addition, the temperature of the inlet water influences the heat transfer performance more than the flow rate. Furthermore, they found that a big amount of energy was charged in a horizontal elliptical tube rather than a little amount in a circular tube. However, a high amount of energy was charged in a bottom eccentric circular tube rather than a top eccentric circular tube.

Jasim et al. [28] investigated the performance of PCM in a triplex-tube storage system with nanoparticles and fins for discharging period. The PCM was placed in the space between the inner and middle tubes (the inner tube diameter was about 50.8mm, and the middle tube diameter was about 150mm) with hot water circulating inside both the inner tube and the annulus between the middle and outer tubes (outer tube diameter was about 200mm). The enthalpy-porosity method was used to discretize the governing equations. The impact of utilizing fins alone, nanoparticles alone, or a combination of the two on discharging operation was studied. They discovered that using fins alone reduces the time required to completely solidify the PCM by up to 55%, using nanoparticles alone reduces the time required by 8%, and combining fins and nanoparticles together reduces the time required by 30%.

Al-Mudhafar et al [29] carried out a numerical investigation to improve the thermal performance of the PCM thermal energy storage system by utilizing a webbed tube heat exchanger in a two-dimensional domain. The webbed tube consisted of four horizontal inner tubes joined together by welded metal plates to increase the surface area of heat transfer. Water as HTF passes through the inner tubes, while the shell side includes the (RT82) as PCM. The governing equations of momentum, continuity, and energy were solved by using the finite-volume method implemented in ANSYS software. They found that the total melting time decreased as a result of an increase in the heat transfer area in the webbed tube exchanger. Furthermore, it was observed that compared to traditional heat exchangers, the webbed tube heat exchanger greatly increases the thermal performance of PCM.

Mahdi et al. [30] conducted a numerical investigation to study the influence of the phase change material location during the charging and discharging cycles on the thermal behavior of the LHTES unit in horizontal shell-and-tube heat exchanger type by using two different models. The first model was the paraffin wax RT 50 filling shell as PCM while the water as heat transfer fluid flows through the tube. The second model was the paraffin wax filling tube as PCM while the water as heat transfer fluid flows through the shell. The study was carried out in the two-dimensional computational domain by using enthalpy method and Boussinesq approximation implemented in the ANSYS Fluent 15 software. The numerical simulation was displayed for melting and solidification at initial temperature 70 ℃, 30 ℃ respectively. They found that the charging time for a second model decreased which was caused by high impact of convection up to 50% when compared with that of the first model. Thermal conduction dominated the beginning of charging for two models then after that changing controlling to free convection. They observed that the increasing inlet temperature of water in both models leads to significantly increased temperature divergence between PCM and HTF. Additionally, at initial time the free convection was predominant on the discharging cycle then replace by the conduction which become predominant cycle.

Kalapala and Devanuri [31] investigated an analysis study to improve the performance of a shell-and-tube LHTES system with the effect of several non- dimensional parameters on the melting characteristics of PCM. The shell is filled with PCM while HTF flows through the tube. The main objective was to study the influence of Reynolds, Rayleigh, Stefan numbers, the ratio of tube thickness to shell diameter and the ratio of thermal diffusivities of tube and PCM. The governing equations of the theoretical solution technique utilize the enthalpy porosity method to solve the problem numerically in ANSYS Fluent software and the SIMPLE algorithm was used for pressure-velocity conjugation. They found that the melting time reduced with increasing the Rayleigh number and inlet temperature of HTF. However, the Reynolds number, as well as thickness and material, have little effect on the PCM melting process.

Ghafoor et al. [32] examined the impact of changing the inner tube geometric shapes on the thermal behavior of PCM in the LHTES system. Three geometrical configurations of the inner tube, namely a circular tube, horizontal elliptical tube, and vertical elliptical tube, were investigated for the solidification cycle. The PCM was placed in the annular gap with cold water circulating through the inner tube. The finite volume method was utilized to discretize the governing equations. In order to deal with the liquid-solid interface advancement through time, the enthalpy-porosity formulation method was employed in the ANSYS fluent 19.2 software. They found that the quick convection currents that govern the PCM discharging operation are initially influenced by buoyancy force, then governed by conduction heat transfer, which takes longer to complete. They discovered that the circular tube performs better because of the prolonged heat absorption from PCM via HTF at 66.37 percent efficiency and 14,430 seconds. This is because of the huge area between the center of the tube and the circular wall in comparison to other shapes.

Soni et al. [33] performed a numerical investigation into the heat transfer between the heat transfer fluid, the wall, and the phase change material to enhance the thermal performance of latent heat thermal energy storage (LHTES) systems. The storage system consists of a shell and tube heat exchanger with the paraffin wax as a PCM filling the shell side while the water as HTF flows through the tube. They studied the effects of free convection, inlet temperature of water, inner tube diameter and length of the storage system on the melting time during charging operation. The numerical model was solved in the transient two-dimensional case by combining the finite difference technique with the enthalpy transforming method for the simulation of phase transitions. The unsteady-state governing equations, convection-diffusion terms and convection terms were discretized by using the implicit method, upwind and backward scheme, respectively. They showed that free convection can noticeably enhance the charging operation and decrease PCM′s overall melting time by more than 50% compared to that without convection. They found that the melting time of paraffin wax increases as the inlet temperature of water increases. Also, the increase in the storage system length led to a rapid increase in the melting time along with the rising mass of PCM. Therefore, the melting time increases as the inner tube diameter decreases.

Shen et al. [34] conducted a numerical investigation to study the influence of the radius ratio in a vertical storage unit using two different chains: constant tube radius with changing shell radius and changing tube radius with constant shell radius. The PCM was placed in the annular space of a shell-and-tube LHTES unit with water as HTF circulating through the inner pipe. The simulation was carried out with the ANSYS Fluent 17.2 program. A grid distribution of 30x300 grids was employed with time steps of 0.1 and 0.15 for both the solidification and melting, respectively. To deal with the liquid-solid interface advancement through time, the enthalpy-porosity technique was employed. They found that the ideal radius ratio slightly increases when the total melting and solidification time increases. Also, the best shell-to-tube radius ratio is around five for both chains.

- Table (2.2) shows a summary of the numerical studies.

2.4 Experimental and Numerical Investigations

Jian-you [35] conducted an experimental and numerical investigation on the heat transfer enhancement in the thermal energy storage unit using a triplex concentric tube with phase change material (PCM). The n-Hexacosane material as a PCM was stored inside the middle channel with the inner tube for the passing of the cold heat transfer fluid for the solidification process and the outer tube for the passing of the hot heat transfer fluid for the melting process. The numerical simulation was performed using iteration method for thermal resistance and temperature to test the change in the phase of PCM. The influence of entry fluid temperature and various mass flow rates of HTF for both cold and hot processes were studied. Furthermore, with experimental data the numerical predictions were validated. They observed that inlet temperature of HTF has a significant effect on the time for full solidification and melting. They found that to produce lowest time the inlet temperature should be low and high for solidification /melting respectively. For each charging and discharging operation, it was found that a good match between the numerical and experimental diagrams for mass flow rate, heat transfer and temperature distributions over time.

Hosseini et al. [36] performed an experimental and numerical investigation to study the influences both of the free convection during melting process of paraffin (RT50) as PCM in a shell and high temperature of HTF on the heat transfer enhancement inside a horizontal shell and tube heat exchanger system. The experimental data showed that the melt's forehead appears to be near the HTF tube, and the migration from tube to shell appears to be underway by natural convection. In addition, a large amount of heat is transferred to the PCM melt area at the same time. Moreover, the finite volume method in numerical simulation proved that the entire charging time is reduced by 37% when the inlet temperature for HTF is raised to 80°C.

Longeon et al. [37] carried out an experimental and numerical simulation to study the PCM influence on melting and solidification operations in a vertical double pipe energy storage system. The annulus geometry consists of a shell and tube filled with a paraffin wax RT35 as a phase change material (PCM) and water moves inside the inner tube as heat transfer fluid. The governing equations were discretized by using ANSYS Fluent software in a 2D axisymmetric geometry. The research was conducted in four cases. In the charging process, the heat transfer fluid was used feeding into the tube from the bottom up, then reflecting the process to start from the very top in the charging process. However, discharging followed the same manner. Their study focused on effects of the natural convection on melting zones as a function of temperature considering the injection configuration in PCMs and its implications for heat transfer. Obtained results of experimental/numerical studies showed that the PCM placed in the top parts heated up quicker and had higher gradients as a result of their proximity to the injection. They noticed that the values were very close during the charging process due to the effect of free convection. Further, the opposite occurs during the discharge process. It was also found that the heat transfer fluid injection side must be carefully selected and advised to charge from the top and discharge from the bottom in order to optimize the performance of the storage unit.

Kibria et al. [38] presented an experimental and numerical study of heat transfer and the effects of phase change material in the latent heat thermal energy storage system, which was governed by thermal conduction. A shell and tube heat exchanger make up the LHTES system. A paraffin PCM melting at 61°C was selected as the storage medium filling the shell while the HTF flows through the tube for both melting and solidification cycles. This study was carried out by using temperature and thermal resistance iteration methods, and has been created in order to analyze heat transfer between PCM and HTF for each operation of melting and solidification. Effects of operating conditions and geometrical parameters such as temperature entering of HTF, various mass flow, tube thickness and radii were displayed. Computational predictions for both the charging and discharging processes agree well with the experimental data. They observed that the tube radius produced greater heat transfer rates between HTF and PCM than the thickness parameters. The results indicate that temperature of the inlet water significant influences on the improve performance of PCM storage unit. In addition, the mass flow rate was found to have an insignificant impact on the overall time of charge and discharge.

Hosseini et al. [39] investigated the influence of inlet temperature of water and thermal behavior of the PCM during paraffin melting and solidification in shell-and tube heat exchanger, with the HTF circulating inside the tube and the PCM filling the shell side. Theoretical model was analysis using an enthalpy formulation for finite volume method. Their results showed that raising the inlet water temperature to 80 °C leads to reduces melting times of the phase change material by 37%. Also, theoretical efficiency of the shell and tube storage system in melting and solidification cycles grew from 81.1% to 88.4%. Obtained numerical results showed that convection and conduction are the most common heat transfer methods that control the phase change process. The convection heat transfer dominates charging of a PCM process and the conduction heat transfer which influences discharging of paraffin wax operation.

Kousha et al. [40] Investigated experimental and numerical the heat transfer enhancement technique based on the modification of the storage geometry of a shell-and-tube LHTES unit by tilting the outer surface of the storage container with angles of (0°, 30°, 60°, and 90°) during both charging and discharging processes of a PCM. A paraffin wax (RT35) filled the shell was chosen as PCM while the water was selected as HTF flows inside the tube. Influence of the different parameters such as Reynolds number, slope angle and Stefan numbers were studied and compared with experimental data. The water flow was in the range of the laminar flow with Reynolds number 770.Their results indicated that when the inlet temperature of heat transfer fluid increases, the charging time decreases in synchronism. The experimental and computational results show that increasing the slope angle from0°to90°decreases the mean temperature of the PCM through the initial half of the operation. Furthermore, in the charging operation, the average heat transfer at horizontal systems is greater than that at vertical systems and vice versa in the discharging process.

Seddegh et al. [41] carried out an experimentally and numerically studied thermal behavior of paraffin RT60 as phase change material during melting and solidification processes inside a vertical shell and tube LHTES unit. The water flows through the tube as a HTF while the PCM fills the shell as a storage medium. They observed that the PCM fluid rises to the top of the unit during the charging cycle. In addition, convection currents cause the molten forehead to transport lower in this same cycle. They found that the maximum heat transfer enhancement occurred at the liquid PCM transition to the top of the storage unit for the solidification process due to the buoyancy forces. Furthermore, the solidification front was observed moving in the axial and radial direction at the same time period.

Korawan et al. [42] presented a numerical and experimental investigation to study the effect of different geometries shapes of thermal energy storage units on the paraffin melting operation. Three types of models were selected: shell and tube, shell and nozzle, and shell and reduce .PCM fills the shell while the water flows through the tube as an HTF. The numerical simulation was displayed for Nusselt number, the liquid fraction and temperature distribution in three – dimensional domains by using ANSYS Fluent program. The empiricist work concentrated on the temperature distribution of paraffin melting. The experiments were examined with numerical results that showed good match. They found that melting of wax occurs in the part near the hot wall ،then the wax rises to settle at the top of the model due to the density variations. It was observed that the shell and nozzle system had shown the better time of charging which is 6130 seconds, followed by the shell and tube system which take 8210 seconds while reducer-and-shell system spent an around 12280 seconds.

Siyabi et al. [43] carried out an experimental and numerical investigation to study the influences of slope angle on the thermal behavior of the paraffin wax during the charging process in a vertical cylindrical container storage unit under different operational conditions. The wax RT35 (melting point between 35 and 37 ºC) as phase change material filling the shell side while the water as HTF passing inside the tube. Results were displayed at different angles (0°, 45°, and 90°), inlet temperature of water 60 ºC and the mass flow rate was 120 ml/min. They observed that angles of slope have a significant impact on the charging cycle. They found that to produce the fastest melting rate, the slope angle should be around 45°. Also, the slope angle of 0°has quicker melted of PCM in the axial orientation. However, the opposite was seen at slope angle 90° which PCM melts faster in the radial orientation. Furthermore, the numerical results indicate that the buoyant force had a main role on the melting rate and melting orientation of paraffin wax.

- <u>Table (2.3) shows a summary of the experimental and numerical studies.</u>

2.5 Summary

This chapter presented an extensive review of the previous numerical and experimental studies related to the heat transfer and enhancement techniques employed in PCMs to effectively charge and discharge latent heat energy. Based on the above reviews, it was observed that many numerical and experimental studies have been done on the geometry and configurations of PCM containers and a series of tests on the melting and solidification of PCM in latent heat energy storage systems to evaluate the effects of different parameters such as the inlet temperature and the mass flow rate of the heat transfer fluid on the performance of these systems. Most of the computational studies reported have used the enthalpy method and computational fluid dynamics (CFD) tools such as ANSYS Fluent for most of the numerical studies to design and analyze LHTES systems. From the above literature review and discussion, it is clear that no CFD modeling work exists concerning the problem of melting and solidification of a commercial paraffin wax embedded inside the concentric annulus pipe. However, the phase change problem with a mushy region in a complex geometry, like an annulus formed concentric horizontal cylinders, is a difficult problem to solve numerically. It is also not clear how some authors numerically handled the arbitrary annulus geometries in their models. The present numerical model was able to provide converged results in every instant of time to evaluate and analyze PCM for charging and discharging processes when the fluid flow is laminar and two-dimensional.

Table2.1: Summary of the experimental studies. 1

Reference	*Tested Model*	*Operation Condition and Geometry Specifics*	*Result*
Akgun et al. [14] (2007)	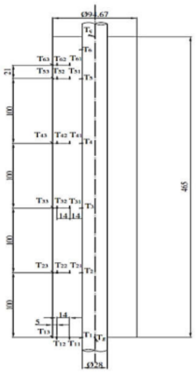	• The concentric conical shell is made of stainless steel and has an inner diameter of 94.67 mm and a length of 465 mm filled with PCM. • Copper tube for water with outer diameter 28 mm. •T-type thermocouples. •32 channel data logger to measurements temperature. •The mass flow rates range of water are: 4,6 and 8 kg/min. •Inner temperature range of water : 60, 65, 70 and 75 °C.	• The total charging time for the 5-degree inclined angle is reduced by approximately 30%. • It was found that the melting time is reduced as the HTF's inlet temperature rises and the mass flow rate decreases.
Rathod and Banerjee. [15] (2014)	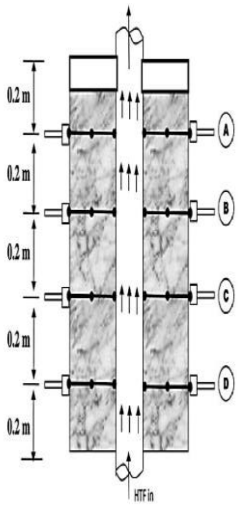	• The vertical concentric shell is made of stainless steel and has an inner diameter of 0.128 m and a thickness of 2.5 mm, with a length of 1 m, which is filled with PCM. • Brass tube with an outside diameter of 0.035 m for water. • Thirty-six thermocouples type-K were distributed to measure the temperatures of the PCM. • The mass flow rate of water ranges from 1-5 kg/min.	• The temperature of the inlet water has a significant influence on the improved performance of the PCM storage unit. •The mass flow rate was found to have an insignificant impact on the overall time of charge and discharge • Melting time needed lower than solidification time. • Convection dominates the melting process, while conduction dominates the discharging process.

Jesumathy et al. [16] (2014)	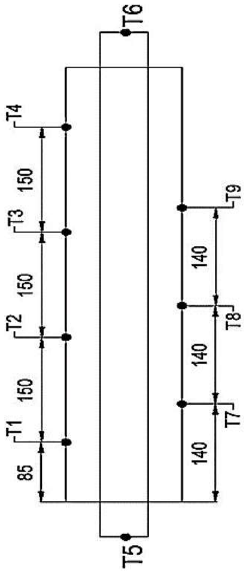	•1.3 kg of PCM is filled into a horizontal mild steel shell with an inner diameter of 98 mm and a length of 620 mm. •A concentric brass tube with a diameter of 50 mm and a length of 780 mm for water. •Insulation made of 30 mm thick asbestos rope. •Nine type-N thermocouples were distributed to measure PCM and inlet and outlet water temperatures. •The mass flow rate of water range: 2, 4, 6, and 8 l/min. •Inlet temperatures range for charging: 70, 72, and 74 ℃. •Inlet temperatures range for discharging: 38, 40, and 42 ℃.	• Convection and conduction were controlling mechanisms for the charging and discharging operations, respectively. • Raising the inlet HTF temperature to 2 °C increased the heat transfer rate during the charging and discharging processes by 25% and 11%, respectively. •Minimized melting time by 31 % through rising entry melt temperature of water from 70 to 74℃. •Minimized solidification time by reduced entry temperature of water.
Shen et al. [17] (2019)	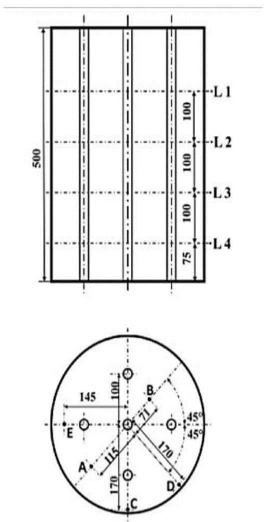	• 35 kg of PCM is filled into a vertical transparent polypropylene concentric shell with an inner diameter of 0.35 m, a 500 mm length, and a thickness of 6 mm. • The fife-oriented copper tube for water has a 19.05 mm outside diameter. • 25 mm thick insulation with 0.036 W/m. K thermal conductivity. • Twenty-two thermocouples T-type. • Inlet temperatures for charging: 80 °C and mass flow rates of 20 l/min. • Inlet temperatures for discharging: 10 °C and mass flow rates of 20 l/min.	• Convection in the melting process was a key factor affecting the heat exchanger's performance. • The PCM solidifies quickly at the lowest position, which is controlled by conduction heat transmission. • The number and placement of tubes in the LHTES units increases the thermal effectiveness of each charging and discharging process.

Kousha et al. [18] (2019)	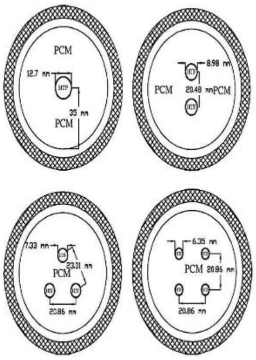	• 1200 g of PCM is filled into a horizontal Plexiglas shell with an inner diameter of 70 mm and a 400 mm length. • Copper tube for water with outer diameter respectively: 12.7, 8.98, 7.33, and 6.35 mm. •Flex elastomeric (ten millimeters thick) was used to insulate the shell. • Sixteen thermocouples J-type. • Water mass flow 0.4 l/min. • Inlet temperatures range for charging: 70, 75 and 80°C. • Numbers of tubes in the shell:1,2,3, and 4. • Inlet temperatures for discharging: 10 °C. • Re number was at the laminar range.	•As the number of tubes increases, heat transfer between the HTF and PCM increases, as does the impact of charging and solidification. • The locations where tubes are distributed have a considerable impact on achieving the best results during processes. •When using 4 tubes and 80℃ of HTF instead of one tube, time for each melting and discharging is reduced by 43 percent and 50 percent sequentially.

Table 2.2: Summary of the numerical studies.

Reference	*Tested Model*	*Operation Condition and Geometry Specifics*	*Results*
Wang et al. [19] (2013)	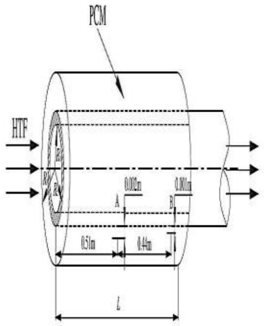	•Horizontal shell having a 0.0258 m outside diameter and a length of 1 m, filled with PCM. •Copper water tube having an outside diameter of 0.0158 m. •The storage container has good insulation. •Range of water mass flow :0.0015-0.0315 kg/sec, and velocity range: 0.0119-0.2514m/sec. •The temperature of the water varies from: 10-60 °C	• The entrance temperature of the HTF has a substantial impact on the charging and discharging processes' completion time. • The flow mass quantity has a significant influence on the charging and discharging processes' completion times. • In the identical conditions of each mass flow rate and temperatures of HTF, discharging has a greater thermal transfer than melting.
Al-Abidi et al [20] (2013)	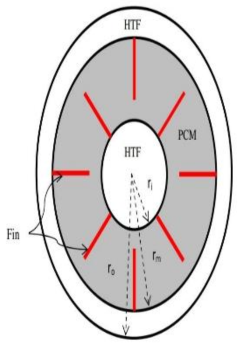	•The inner, middle, and outer tubes have a radius of 25.4 mm, 75 mm, and 100 mm, respectively. •The inner and outer tubes have a thickness of 1.2 mm and 2 mm, respectively. •Max melting temperature was 95°C.	•Fin thickness has a minor impact compared to fin length and number of fins, which have a significant impact on melting rate time. •It is found that the different shapes of storage systems with fins have an effect on the heat transfer enhancement compared with those without fins.

Seddegh et al. [21] (2015)	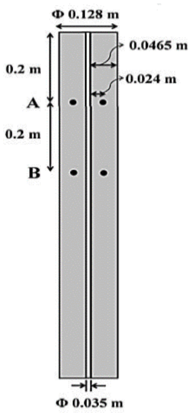	•Vertical shell with outside diameter of 0.128 m which filling with PCM. •Concentric tube for water with diameter of 0.035 m. •Inlet temperatures for melting operation: 358 K. • Inlet temperatures for solidification operation: 301K. •The mass flow 5 l/min with Reynolds number 32152.	• A good harmonize among numerical forecasting and the experimental results published in previous researches. • Thermal conductive/convective type gives the best characterization of thermal performance for PCM than thermal conductivity type. • Thermal conduction controlling discharging process while the natural convection controlling the charging process.
Seddegh et al [22] (2016)	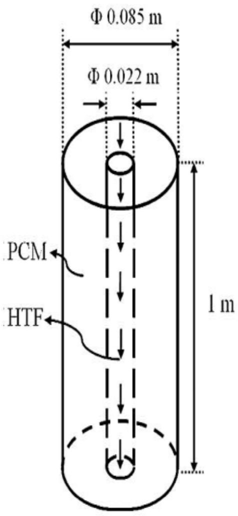	•Vertical copper shell with inner diameter 0.085 m and 1 m length which filling with PCM. •Concentric copper tube for water with outer diameter 0.022 m. •Inlet temperatures for charging process: 343K with mass flow rate of l/min. •Inlet temperatures for solidification operation: 293K	• The results matching the experimental numbers and showed that conduction heat control over discharging in each of the vertical and horizontal equipment. • The active melting in the higher region of PCM better than the bottom region in the horizontal equipment while the similar charging in each point in the vertical equipment. • A low effect on the mass flow rate of water and large influence on the temperature of water for each horizontal/vertical unit

Esapouret.al [23] **(2016)**	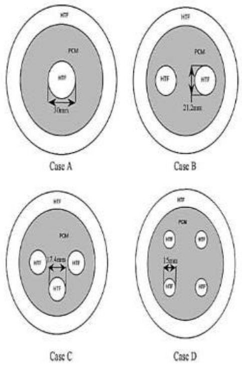	•Horizontal unit with outer diameter tube 125 mm and mid diameter tube 95 mm with 1 m long which filling with PCM. •The inner tube for water which outer diameter change:30, 21, 17.4, and 15 mm. •Water mass flow range: 0.024, 0.032, and 0.04 kg/sec. •Water melts temperature range: 50, 60, and 70 ℃.	• Numerical results showed that the melt time of PCM minimized due to the rising HTF temperatures entry. • There was no high effect Inferred from the mass flow rising of HTF on PCM melting. • The melts time of the PCM decreased as the number of tubes inside the shell increased, reaching 29 percent with shell and four tubes.
Mousavi Ajarostaghi et.al [24] **(2017)**	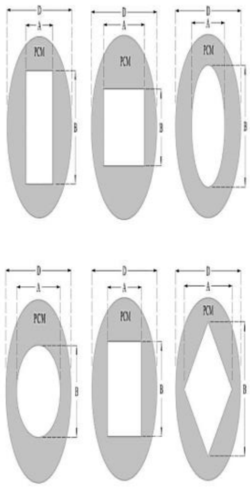	•Circular with outer/inner diameter: 23mm*10.38mm. •Circular outer diameter 23 mm with horizontal of elliptical 13.25 mm*10 mm. •Circular outer diameter 23 mm with vertical of elliptical 10 mm*13.25 mm. •Circular outer diameter 23 mm with horizontal of rectangular 25 mm*16.61 mm. •Circular outer diameter 23 mm with vertical of rectangular 16.61 mm*25 mm. •Circular outer diameter 23 mm with square 10.38 mm*10.38 mm. •Circular outer diameter 23 mm with diamond 10.38 mm*10.38 mm.	• Thermal conduction at the charging operation was the main control for all-region, afterward the natural convection control at 50 percent of the upper region. • Best geometric shapes for quickly charging PCM was vertical rectangular, vertical elliptical, square, and diamond shape respectively from others. Also, the vertical rectangular shape has 74 percent reducing charging time compared with a circular shape. • The horizontal rectangular shape has weaker charging specifications from other shapes .

Han et al [25] (2017)	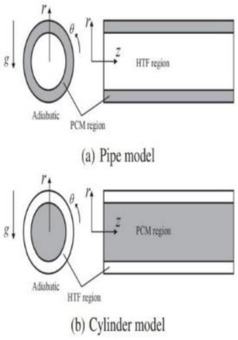	• Horizontal / vertical pipe model with an inner tube diameter of 20mm for water and an outer tube diameter of 28.28mm filled with PCM. • Horizontal/vertical cylinder model has a 500 mm length, an inner tube diameter of 20 mm, and is filled with PCM and outer tube diameter 28.28 mm for water. •Inlet temperature of HTF is 573 K. •Inlet velocity of HTF is fixed at 15 m/s.	• The PCM melting rate in the horizontal cylinder model was improved by the effect of natural convection more than in the horizontal pipe model. •They reported that the time it takes to finish the melting process has been lowered by 23.5 %. • The vertical pipe model with an HTF input at the lower had the maximum PCM melting rate, in contrast to the horizontal and vertical cylinder models where the HTF inlet at the lower is nearly the same.
Elmeriah et al. [26] (2018)	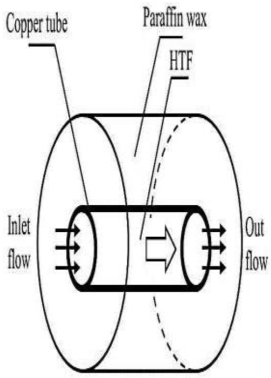	•Horizontal shell with 1 m long and inner diameter 0.036 m which is filled with paraffin wax. •Double copper tube for water with outer diameter 0.012 m. •The storage system is insulated. •Inlet temperatures for charging operation: 88°C with mass flow 0.072kg/min. •Inlet temperatures for discharging operation: 25°C with mass flow 0.07 kg/min. •Reynolds number range: 100-1500	• A good match between numerical forecasts and experimental data from prior studies. •Reynolds numbers have a significant effect on the time and rate of the changing and discharging operations. • The shell diameter and tube length are the most effective parameters which improve the storage system performances and have a major effect on the exit temperature of water.

Begum et al. [27] (2018)	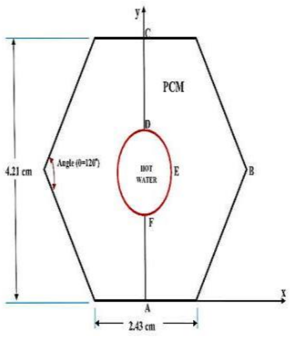	•Horizontal hexagonal shell with a height of 4.21 cm and a length of 2.43 cm, filled with paraffin wax. •The water flows inner tube cross-section changes: concentric circular tube with inner diameter 1.7 cm, upper and lower eccentric tube, horizontal elliptic, and vertical elliptic. •The storage unit is insulated. •charging and discharging temperature of PCM 59.9°C/51.2°C, respectively. •Mass flow rate range: 0.01-0.04 kg/sec.	•The natural convection affects the melting of the wax in the upper part of the test system more than the wax in the lower part of the test system because of the buoyancy force. •The temperature of the inlet water influences the heat transfer performance more than the flow rate. • A big amount of energy was charged in a horizontal elliptical tube rather than a little amount in a circular tube.
Jasim et al. [28] (2018)	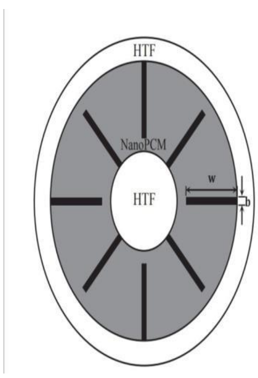	• Three copper tube with long 500mm. •Inner tube for water with diameter 50.8 mm and thickness 1.2mm. • Middle tube filled with PCM and diameter 150mm, thickness 2mm. •Outer tube for water with diameter 200mm and thickness 2mm. •Solidification temperature 350 K	• They discovered that using fins alone reduces the time required to completely solidify the PCM by up to 55%. • using nanoparticles alone reduces the time required by 8%, and combining fins and nanoparticles together reduces the time required by 30%.

Al - Mudhafar et al [29] **(2018)**	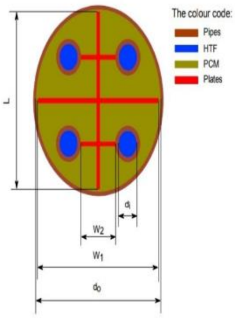	• Horizontal four tubes with inner diameterv20mm and thick 3 mm. • Shell with inner diameter 150mm and thick 2mm, filled by PCM. •Plates length 144 mm and width one 144mm and width two 26.5mm with thick 3mm. •Copper was made for tubes and plates.	•The total PCM melting time decreased as a result of an increase in the heat transfer area in the webbed tube exchanger. •It was observed that compared to traditional heat exchangers, the webbed tube heat exchanger greatly increases the thermal performance of PCM.
Mahdi et al **[30]** **(2019)**	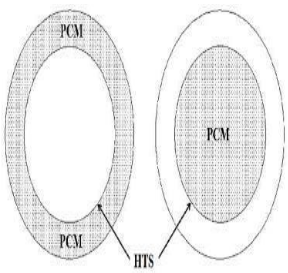	•Horizontal shell with a 7.07 cm inner diameter. • 5 cm inner diameter double tube. •Using the first model, the tube for water and the shell for PCM and the second model the inverse. •Inlet temperatures range for charging cycle: 70, 75, and 80°C. •Inlet temperatures range for discharging cycle: 20, 25, and 30 °C	•The charging time for a second model decreased which was caused by high impact of convection up to 50% when compared with that of the first model. • Conduction dominated the beginning of melting for two models then after that melting control to free convection. •At initial time the free convection was predominant on the solidification cycle then replaced by the conduction which became the predominant cycle.

Kalapala and Devanuri. **[31]** **(2019)**	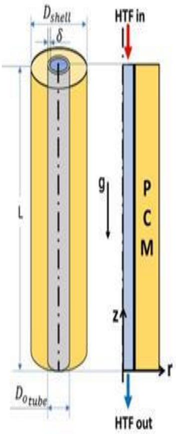	•Vertical shell with inner diameter 44mm which filling with PCM. •Double tube for water with outer diameter 17.5mm. •Well outer shell insulation. •Stefan number range :0.2–0.6 •Reynolds number range :500–2000. •Rayleigh number range :(2.04 × 10^5–2.32 × 10^6. • Tube thickness to diameter ratio: 0.036–0.113. •L/D ratio :1–10. •Thermal diffusivity ratio :45.29–1500.	•The melting time is reduced with increasing the Rayleigh number and inlet temperature of HTF. •Reynolds number as well as thickness and material of tube have little effects on the PCM melting process.
Ghafoor et al. [32] **(2020)**	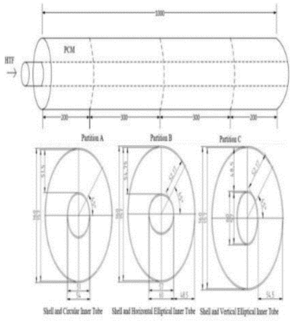	• Geometric shapes selected consist of: •Horizontal shell with 1000mm long ,thickness 1.5mm and outer/inner diameter 160,157mm which filling with PCM. • Copper circular tube for water with 1500mm long,1.5mmthickness and outer /inner diameter 54,51mm. •Horizontal elliptical tube with inner diameter 47.5mm and outer diameter 60mm. •Vertical elliptical tube with inner diameter 47.5mm and outer diameter 60mm. •Angle range: 0° ,45° and 90° .	•They found that the quick convection currents that govern the PCM discharging operation are initially influenced by buoyancy force, then governed by conduction heat transfer, which takes longer to complete. • The circular tube performs better because of the prolonged heat absorption from PCM via HTF at 66.37 percent efficiency and 14,430 seconds. This is because of the huge area between the center of the tube and the circular wall

Soni et al. **[33]** **(2020)**	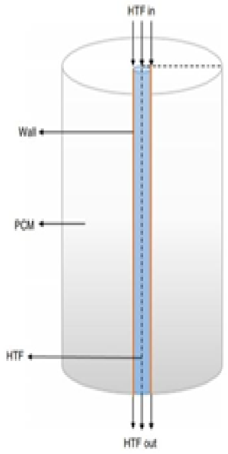	•Brass shell with inner diameter 128mm filling with PCM and external insulation. •Copper tube for water with inner diameter respectively: 15, 25 and 33 mm. •Vertical storage system with long :1, 2 and 3m. •Inlet temperature of HTF range :45, 55 and 65 °C. •Inlet velocity of water: 0.02 m/s.	in comparison to other shapes. They showed that free convection can noticeably enhance the charging operation and decrease PCM overall melting time by more 50% compared to that without convection. •The melting time of paraffin wax increases as the inlet temperature of water increases. •The increase in the storage system length led to a rapid increase in the melting time along with the rise mass of PCM. •The melting time increases as the inner tube diameter decreases.
Shen et al. **[34]** **(2020)**	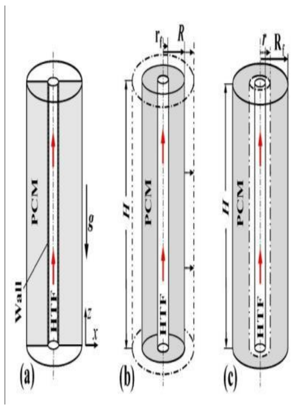	•First chain: varying shell radius (25.4,50,8,63.5,76.2 and 101.6mm) with constant tube radius of 12.7mm. •Second chain: varying tube radius (25.4,15.9,9.5 and 7.1mm) with constant shell radius of 63.5mm. •Both chains have two heights 600,1200mm. •Copper tube for water with thickness 1.2mm. •Inlet velocity of HTF is 0.201m/s and Reynolds number 7010.	• They found that the ideal radius ratio slightly increases when the total melting/solidification time increases. • The best shell-to-tube radius ratio is around five for both chains.

Table 2.3: Summary of the experimental and numerical studies.

Reference	***Tested Model***	***Operation Condition and Geometry Specifics***	***Results***
Jian-you [35] **(2008)**	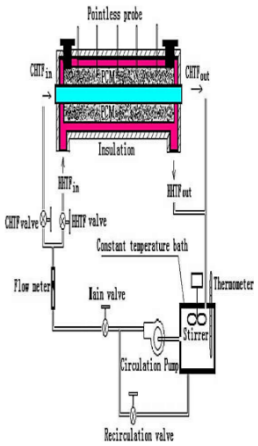	• Three copper tubes are triplex concentric and the outer wall insulated by a 20 mm thick Styrofoam layer. •The inner tube for hot water with inside diameter of 90 mm and outside diameter of 94 mm with 3040 mm length. •The middle tube fills PCM with an inside diameter of 80 mm and outside diameter of 82 mm with 3000mm length . •The outer tube for cold water with inside diameter of 15 mm and outside diameter of 17 mm with 3100 mm length . •16 thermocouples from a copper constant (Type T) were used to calculate PCM temperatures. •Scope of water mass flow:0.05-2 l/min. •Inlet fluid temperatures for melting: 58 °C. •Inlet fluid temperatures for solidification: 23 °C.	• The numerical simulation was performed using an iteration method for thermal resistance and temperature to test the change in the phase of PCM. • The inlet temperature of HTF has a significant effect on the time for full solidification and melting. • for each charging and discharging operation, it was found that a good match between the numerical and experimental diagrams for mass flow rate, heat transfer, and temperature distributions over time.
Hosseini et al. [36] **(2012)**	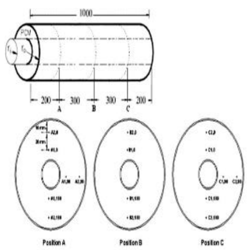	•A 1 m in length horizontal tube formed of 2.5 mm thick iron with an interior diameter of 85 mm served as the 4 Kg PCM filling storage. •22 mm outside diameter concentric copper tube transporting hot water. •Insulation made of glass wool with a 60mm thickness. •There were 18 type-K thermocouples distributed to take temperature readings and keep track of them in the PCM. •Water mass flow: 1 l/min. •Melting temperatures range at the inlet are :70, 75, and 80 °C.	•The experimental data showed that the melt's forehead appears to be near the HTF tube, and the migration from tube to shell appears to be under way. By natural convection, a large amount of heat is transferred to the PCM melt area at the same time . •The finite volume method in numerical simulation proved that the entire charging time is reduced by 37% when the inlet temperature for HTF is raised to 80°C.

Longeonal et al. **[37]** **(2013)**	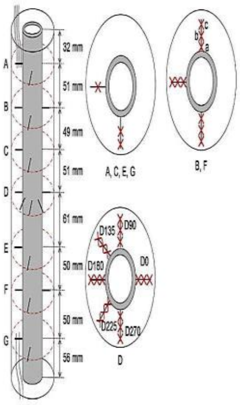	• The storage unit is composed of two concentric cylinders 400 mm long. • one vertical plexiglas with an inner diameter of 44 mm which the annular space is filled by 480 g of PCM. •other cylinder stainless steel for water as HTF with inner diameter of 15 mm and thick of 2.5 mm. • 48 thermocouples type-K were distributed to measure the inlet and outlet temperature of HTF. • Less than 2300 Reynolds number so the flow was taken laminar with constant velocity 0.01m/sec.	• They noticed that the values were very close during the charging process due to the effect of free convection. • The values of both experimental and numerical opposite occur during the discharge process. • They found that the heat transfer fluid injection side must be carefully selected and advised to charge from the top and discharge from the bottom in order to optimize the performance of the storage unit.
Kibria et al. **[38]** **(2014)**	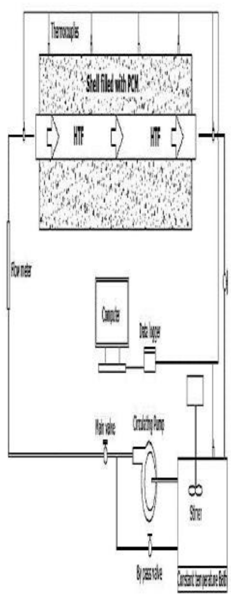	• 1 m long copper shell filled with paraffin wax with an inner diameter of 36 mm. • double copper tube with inner diameter 10.8 mm and outer diameter12.0 mm with water flowing through it. insulated by a styrofoam layer 20mm thick. • thermocouples (type RTD) to measure entry /exit temperature of HTF and PCM. • Entry temperatures for charging: 88 °C and mass flow 0.072 kg/min. • Entry temperatures for discharging: 25 °C and mass flow 0.07 kg/min.	• Computational predictions for both the charging and discharging processes agree well with the experimental data. • They observed that the tube radius produced greater heat transfer rates between HTF and PCM than the thickness parameters. • The temperature of the inlet water influences the heat transfer performance of the PCM storage unit. • The mass flow rate was found to have an insignificant impact on the overall time of charge and discharge .

Hosseini et al. [39] **(2014)**	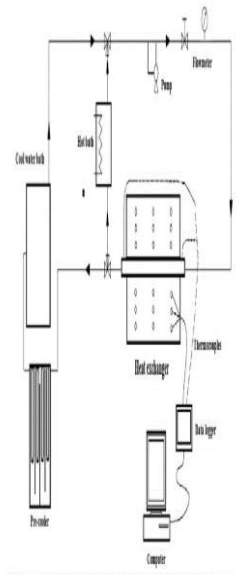	• 1 m long horizontal shell-and-tube latent heat thermal energy storage system. • Double copper tube for heat transfer fluid (water) with outer diameter 22 mm. • copper shell filling 4 kg paraffin RT50 with inner diameter 85mm. Glasswool insulation with a thickness of 60 mm. • Eighteen thermocouples type-K. • Entry temperatures range for charging :70, 75, and 80 °C and mass flow 1 l/min. • Entry temperatures for discharging: 25 °C and mass flow 1 l/min.	• Raising the inlet water temperature to 80 °C leads to reduced melting times of the phase change material by 37%. • theoretical efficiency of the shell and tube storage system in melting and solidification cycles grew from 81.1% to 88.4%. • The convection heat transfer dominates charging of a PCM process and the conduction heat transfer which influences discharging of paraffin wax operation.
Kousha et al. [40] **(2017)**	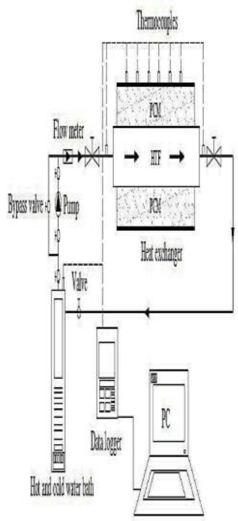	• Storage system consists of two cylinders and the space between them is filled with paraffin RT35 as PCM. • 400 mm long Plexiglas shell with inner diameter 70 mm. • Double copper tube for passing water as HTF with outer diameter 12.7 mm. Flex elastomeric insulation with 10mm thick. •Sixteen thermocouples J-type. •Inlet temperatures range for charging: 70,75, and 80 °C and mass flow 0.4 l/min. •Slope angle range:0, 30, 60, and 90. •Reynolds number: 770.	•When the inlet temperature of heat transfer fluid increases the charging time decreases in synchronism. • Increasing the slope angle from 0° to 90° decreases the mean temperature of the PCM through the initial half of the operation. • In the charging operation, the average heat transfer at horizontal systems is greater than that at vertical systems and vice versa in the discharging process.

Seddegh et al [41] **(2017)**	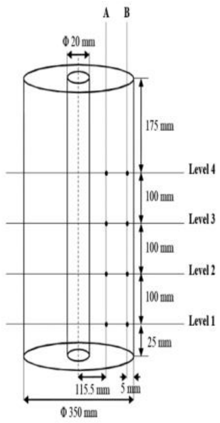	• vertical cylindrical thermal storage unit with 0.5 m length. • polypropylene transparent shell with inner diameter 0.35 m filling with 25 kg paraffin wax. • Double copper tube for water as HTF with outer diameter 20 mm. •Thermocouples type-T were used. • Insulated by using an Armaflex sheet with thermal conductivity of 0.036 W/m ·K.	• They observed that the PCM fluid rises to the top of the unit during the charging cycle while convection currents cause the molten forehead to transport lower in this same cycle. • The maximum heat transfer enhancement occurred at the liquid PCM transition to the top of the storage unit for the solidification process due to the buoyancy forces. • The solidification front was observed moving in the axial and radial direction at the same time period.
Korawan et al. **[42]** **(2017)**	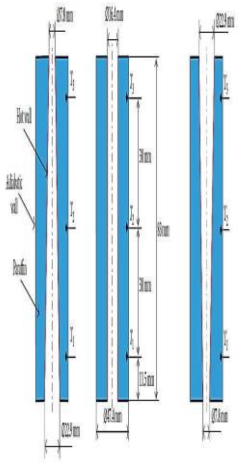	• Vertical copper nozzle for water flows through the tube with small diameter 7.8 mm and large diameter 22.9 mm and 0.5 mm thickness. • Shell made of PVC with inner diameter 47.4 mm and 83 mm length filling with PCM. • Two models have been included for numerical analysis: a tube with an outer diameter of 16.4mm and a reducer with a small diameter of 7.8 mm and a big diameter of 22.9 mm. • The system is insulated by Styrofoam with 10 mm thickness. • Five thermocouples were distributed to measure HTF and PCM temperatures. •Inlet temperatures for charging operation: 330 K and 301K initial temperature of wax.	• The experiments were examined with numerical results that showed good match. • The melting of wax occurs in the then the wax ‹part near the hot wall rises to settle at the top of the model due to the density variations. • The shell and nozzle system had shown the better time of charging which is 6130 sec, followed by the shell and tube system which take 8210 seconds while reducer-and shell system spent an around12280 seconds.

Siyabi et al. [43] **(2019)**	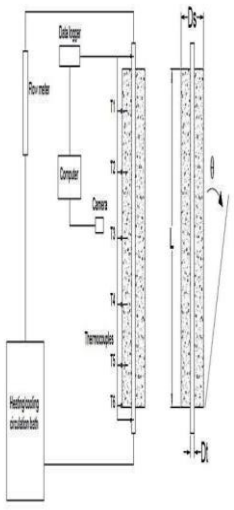	• Vertical cylindrical storage system consists of a shell and tube heat exchanger. • Shell with inner diameter 40 mm and 183mm length which is filled with 170 g paraffin wax. • Double copper tube for water as HTF with inner diameter 8 mm and 2 mm thickness. •Eight thermocouples type-K were distribution to measure PCM and HTF temperatures. •Entry temperatures for melting operation: 60°C with mass flow 120 ml/min. • The slope range of angles: 0°, 45°, and 90°.	• The angles of slope have a significant impact on the charging cycle and to produce the fastest melting rate, the slope angle should be around 45°. •The slope angle of 0°has quicker melted of PCM in the axial orientation. • The PCM melts faster in the radial orientation at slope angle 90°. • The numerical results indicate that the buoyant force had a main role on the melting rate and melting orientation of paraffin wax.

CHAPTER THREE

Mathematical Model and Numerical Solution

3.1 Introduction

This chapter describes the mathematical model and procedure of the numerical solution used in the current study. The first part explains the physical model description and assumptions of this study. However, the governing equation of the laminar flow in the form of cylindrical coordinates and the boundary conditions for all dependent variables are presented, as well as the thermophysical properties of the utilized materials are included. Moreover, the procedure of the numerical solution begins with the discretization of the governing equations, which were illustrated in the next part by using the enthalpy-porosity method. The computational grid and mesh dependency are presented as well. CFD technology was utilized the ANSYS software package for dealing with fluid flows (FLUENT) to simulate the present problem.

3.2 Research methodology

In the current study, the arrangement of geometry essentially consists of two pipes, one inner tube subjected to a constant temperature and the other an insulated outer shell pipe. A transient two-dimensional cylindrical coordinate axi-symmetry in computational fluid dynamics (CFD) model has been developed to simulate the thermal behavior of PCM during the melting and solidification processes using a commercial software package (ANSYS FLUENT 2020 R2). The model geometry is built by using Design Modeler. Then, the model geometry is meshed to split the domain into sub domains (i.e., cells or elements) using a square mesh. However, when the geometry is created, the mesh is constructed and boundary conditions are prescribed.

Many meshes are examined in order to get an appropriate grid system. This is well known as the "grid independence test" (GIT). An intensive mesh takes a long time to simulate the case, while the low-density mesh provides incorrect results. As a result, the GIT limits the mesh density and saves solution time. In order to obtain an accurate result after doing GIT, the results are validated with the pertinent results of the study. Three important stages of FLUENT-CFD analysis are implemented as follows: The first stage, which is called "pre-process stage", which involves generating and developing the geometrical shape as well as meshing of the studied geometry and adjusting the boundary conditions. The second step called "solver stage" or "processing stage", which includes solving the applied governing equations. Finally, the "post-processing step" includes the simulated results and representation of these results via graphics, plots and animations. The approach flowchart of this research is presented in Figure 3.1.

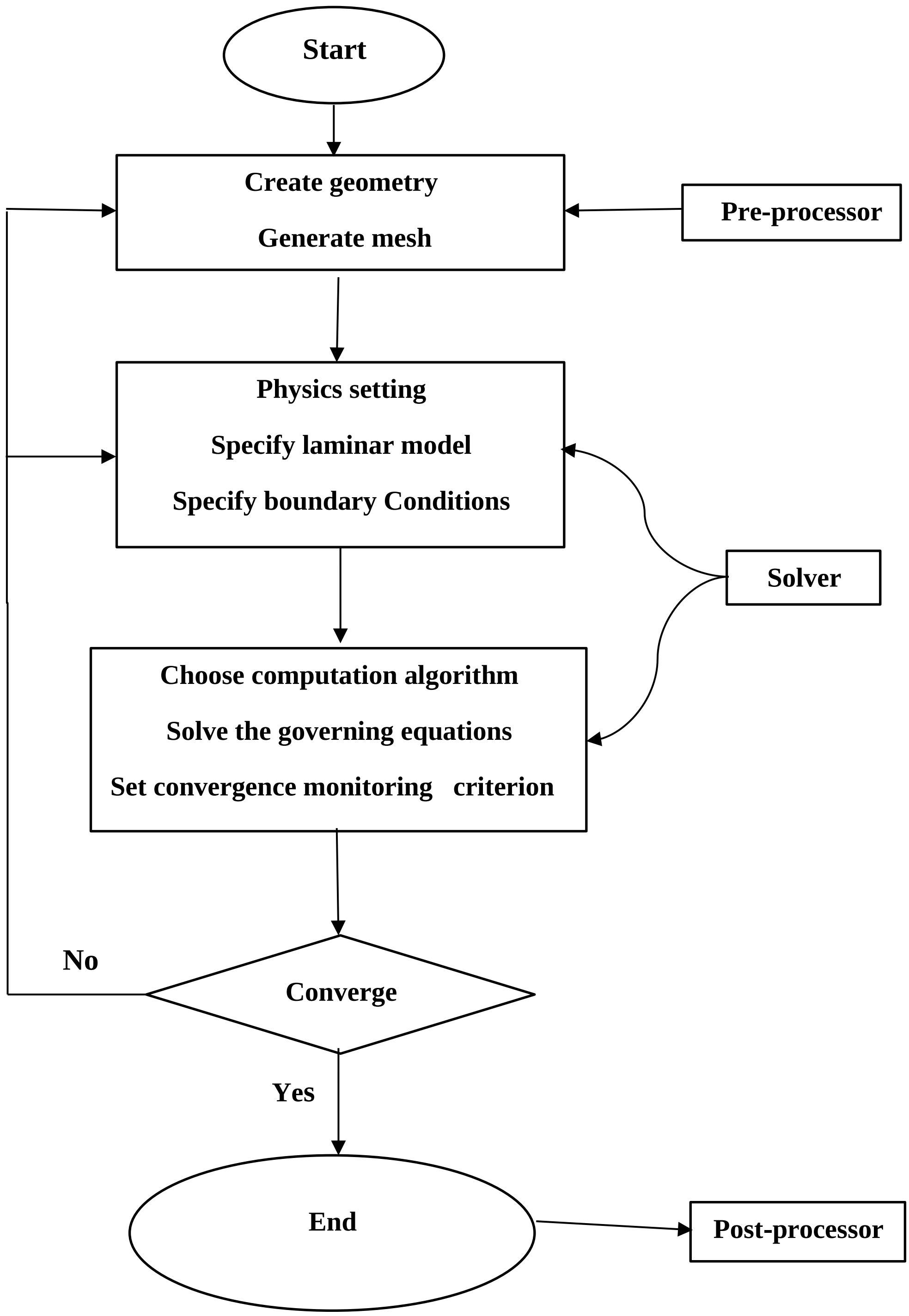

Figure 3.1: Flow chart of the numerical study

3.3 Model Description

The basic geometry of the horizontal shell-and-tube LHTES system, which consists of two concentric pipes, is shown in Figure 3.1. The inner tube has an internal diameter of (51 mm) and an external diameter of (54 mm), while the outer shell has an internal diameter of (157 mm) and an external diameter of (160 mm). The inner pipe is made up of copper, whereas the outer pipe is made up of aluminum. Table 3.1 presents the dimensions of these pipes and the types of materials that are used in the model. The annulus is filled with paraffin wax as PCM while water as HTF flows through the inner pipe. During the melting process, hot HTF is circulated through the inner pipe. Cold HTF is circulated through the inner pipe during the solidification process. Hot water enters the storage system at 67°C during the charging operation. Cold water enters the storage system at 27°C during the discharging operation**.** Due to symmetry in the θ-direction, the computation has been conducted on the right-half of the domain**.**

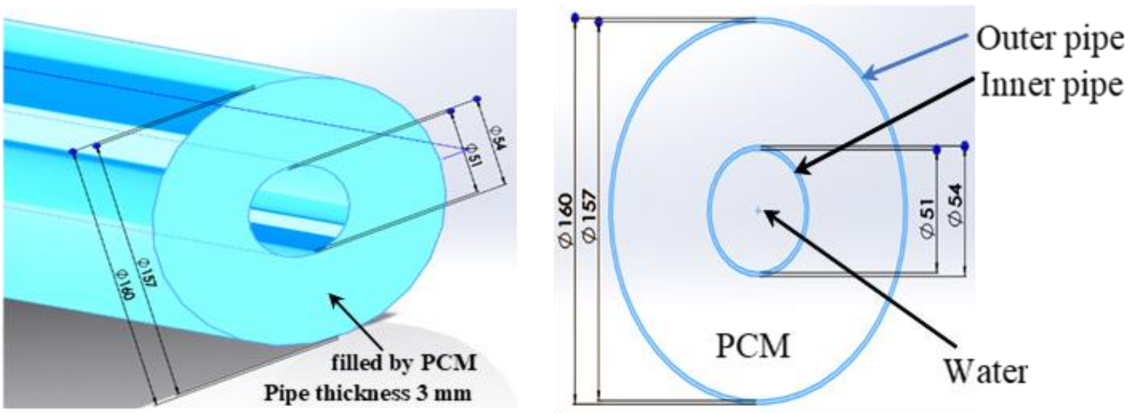

(a) (b)

Figure 3.2. Schematic of the concentric annulus pipes: (a) 3D view, (b) Cross section view.

Table 3.1: Dimensions and materials of the concentric pipes.

Parameters	Diameters		Materials
	Internal	External	
Inner pipe	51 mm	54 mm	Copper
Outer pipe	157 mm	160 mm	Aluminium

3.4 Thermophysical Properties and Assumptions

The thermophysical properties of PCM, water, aluminum and copper that utilized in the numerical study are shown in Table 3.2. The main assumptions of phase transitions and fluid flow can be defined as follows:

1) A laminar flow, incompressible, Newtonian fluid, unsteady and two-dimensional flow.
2) The PCM is isotropic and homogeneous.
3) The outside shell pipe's surface is insulated.
4) The HTF inlet temperature is fixed at 300 K.
5) Boussinesq approximation is implemented to buoyant force and density.

Table 3.2: Thermophysical properties of used materials [32].

Property	PCM	Water	Aluminum	Copper
Melting temperature [K]	334			
Density in solid state [kg/ m^3]	894.56		2719	8978
Density in liquid state [kg/m^3]	783.42	998.2		
Specific heat in solid state [J/kg K]	1659		871	381
Specific heat in liquid state [J/kg K]	2460	4182		
Latent heat of fusion [J/kg]	235512.5			
Thermal conductivity in solid state [W/m K]	0.259		202.4	387.6
Thermal conductivity in liquid state [W/m K]	0.158	0.6		
Dynamic viscosity [kg/m s]	0.01405	0.001003		
Solidus temperature [K]	318.5			
Liquidus temperature [K]	339			
Thermal expansion coefficient [1/K]	0.000307			
Density [kg/m^3]	2621.3-5.4215T			
Specific heat capacity [kJ/kg. K]	-10786+39.073T			
Thermal conductivity [W/m. K]	1.8282-0.0049268T			

The material properties of density, specific heat capacity and thermal conductivity were represented as a function of the temperature in a set of linear equations. Depending on the PCM temperature range between each of the liquid-state and solid-state. The temperature range was 300 K < T < 350 K of the PCM. Table 3.3 shows the result of the thermophysical properties of PCM.

Table 3.3: Thermo-physical Properties of PCM in Temperature Range 300K < T < 350K.

Temperature (K)	*Density (kg/m^3)*	*Specific heat (kJ/kg. K)*	*Thermal conductivity (W/m .K)*
300	994.85	935.9	0.35016
305	967.7425	1131.265	0.325526
310	940.635	1326.63	0.300892
315	913.5275	1521.995	0.276258
320	886.42	1717.36	0.251624
325	859.3125	1912.725	0.22699
330	832.205	2108.09	0.202356
335	805.0975	2303.455	0.177722
340	777.99	2498.82	0.153088
345	750.8825	2694.185	0.128454
350	723.775	2889.55	0.10382

3.5 Governing Equations

The enthalpy-porosity approach [44,45] applied in Fluent software was employed to consider the phase change phenomenon. It is used because of its capacity to simplify explicit tracking of the solid-liquid interface and proving a simple procedure for phase-change problems [46,47 and 48]. This method provides the most accurate simulation results as well as the most accurate visualize image of the active operations. The followings are the benefits of this technique:

- Multi-dimensions and numerical solution.
- It is updated and more accurate.
- The enthalpy components at a mushy zone contain a mixture of each liquid and solid materials.
- The governing equations similar to the single-phase equation.
- No explicit conditions are needed to be satisfied the solid-liquid interface.
- All researchers depend on it now [49,50].

Numerical models were performed to simulate the cases in this work, according to the following steps, which are:

- Modeling the required geometry.
- Mesh the geometry.
- Write the correlations, materials, conditions of cell zone and boundary conditions, solution procedure and control.
- Analysis of the finding and post-processing.

The conservation equations governing the problem of phase change [22], these equations are displayed in detail in the following:

Continuity equation:

$$\frac{\partial \rho}{\partial t} + \nabla \cdot (\rho \vec{v}) = 0 \qquad (3.1)$$

Momentum equation:

$$\frac{\partial \rho v}{\partial t} + \nabla \cdot (\rho \vec{v}\, \vec{v}) = -\nabla P + \nabla \cdot (\mu \nabla \vec{v}) + \rho g + \frac{(1-f)^2}{f^3+\varepsilon} \vec{v} A_{mush} \qquad (3.2)$$

Energy equation:

$$\frac{\partial \rho H}{\partial t}\ \nabla \cdot (\rho \vec{v} H) = \nabla \cdot (k\, \nabla T) + S \tag{3.3}$$

The enthalpy is as follows:

$$H = h + f\ L \tag{3.4}$$

$$h = h_{ref} + \int_{T_{ref}}^{T} C_P\ dT \tag{3.5}$$

where (f) is the liquid fraction:

$$f = \begin{cases} 0 & T < T_{Solidus} \\ \dfrac{T - T_{Solidus}}{T_{Liquidus} - T_{Solidus}} & T_{Solidus} \leq T \leq T_{Liqudus} \\ 1 & T > T_{Liquidus} \end{cases} \tag{3.6}$$

Rearranging the energy equation by applying equations (3.4), (3.5) and (3.6) into eq. (3.3) gives:

$$\frac{\partial \rho h}{\partial t} + \nabla \cdot (\rho \vec{v} h) = \nabla \cdot (k\, \nabla T) - \frac{\partial \rho f L}{\partial t} - \nabla \cdot (\rho \vec{v} f L) + S \tag{3.7}$$

The Boussinesq approximation [52,53] was used to account for the buoyancy force driving the fluid's convective motion. The density is considered to be constant throughout the governing equations, with the exception of the buoyancy element. The density variation is defined as:

$$\rho = \rho_0 \left(1 - \beta\, (T - T_0)\right) \tag{3.8}$$

By substituting eq. (3.8) in eq. (3.2), the momentum equation can be expressed as follows:

$$\frac{\partial \rho_0 \vec{v}}{\partial t} + \nabla \cdot (\rho \vec{v}\, \vec{v}) = -\nabla P + \nabla \cdot (\mu\, \nabla \vec{v}) + (\rho - \rho_0) g + \frac{(1-f)^2}{f^3 + \varepsilon} \vec{v} A_{mush} \tag{3.9}$$

The term A_{mush} is the mushy zone constant and the value in this study is used as 10^5,ε is a tiny number (0.001) to avoid a zero division. (ρ_0), (T_0) are operating density and temperature.

3.6 Boundary and Initial Conditions

In order to discretize the governing equations, the boundary conditions for all dependent variables should be defined at all boundaries of the computational domain. Due to symmetry, the solution domain is selected as the right-half of the annulus. The PCM is initially set to liquid with a temperature of 67°C during the solidification process and set to solid with a temperature of 27°C in the melting process. The HTF temperature is 27°C for solidification process and 67°C for melting process. Thermal conditions of the outer pipe insulated (adiabatic) and the inner pipe at constant temperature (isothermal). The boundary conditions are explained in Figure 3.2.

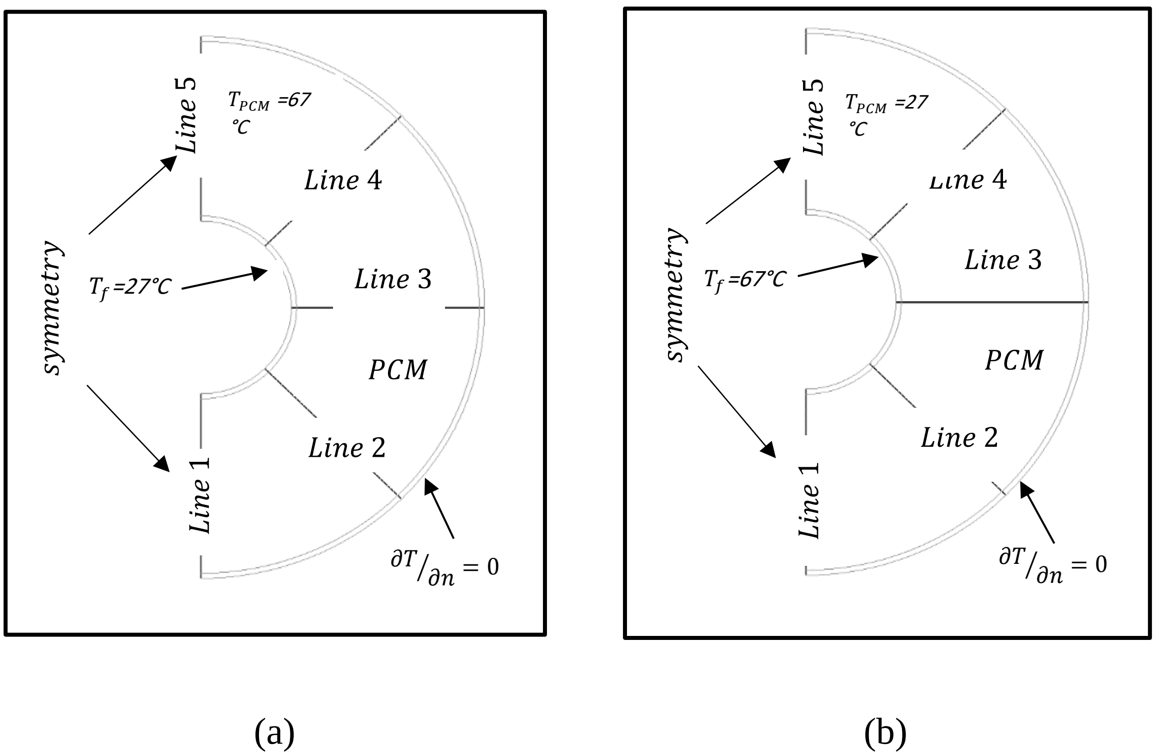

Figure 3.3. Computational domain with boundary conditions: (a) Solidification process, (b) Melting process.

3.7 Numerical Solution and Mesh Dependency

The numerical simulation of the transient two-dimensional problem was executed based on finite volume method. The current problem is solved numerically utilizing the CFD program, FLUENT 20. The pressure-velocity coupling correlations were simplified with utilizing the Semi-Implicit Pressure-Linked Equation (SIMPLE) algorithm and the correction correlation of the pressure was simplified using the PRESTO scheme. A quick differencing scheme is conducted to discretize the convection terms of the momentum and energy equations while the diffusive terms have been discretized using central difference scheme. Tables 3.4 and 3.5 show the grid sizes studied to validate the numerical solution for grid size independence. The number of nodes that was employed in this study (315601). Each time step has a number of steps be 300 and the time step is set to 0.001s. Mesh dependency applied to present case study for solidification process during transient solution after 3 hours according to PCM average temperature PCM liquid fraction.

Table 3.4: Mesh dependency in the present study for PCM average temperature after 3 hours of solidification process.

No. of nodes	256478	290865	312323	315601	326145	358213
Line 1	26.31482	37.5926	41.76956	42.622	42.83511	42.40676
Line 2	30.35262	43.36088	48.17876	49.162	49.40781	48.91373
Line 3	32.69195	46.70278	51.89198	52.951	53.21576	52.6836
Line 4	35.22267	50.3181	55.909	57.05	57.33525	56.7619
Line 5	36.11852	51.59788	57.33098	58.501	58.79351	58.20557

Table 3.5: Mesh dependency in the present study for PCM liquid fraction after 3 hours of solidification process.

No. of nodes	256478	290865	312323	315601	326145	358213
Line 1	0.158208	0.226012	0.251124	0.279027	0.279585	0.279306
Line 2	0.158208	0.226012	0.251124	0.279027	0.279585	0.279306
Line 3	0.237691	0.339558	0.377287	0.419208	0.420046	0.419627
Line 4	0.341567	0.487953	0.54217	0.602411	0.603616	0.603013
Line 5	0.378334	0.540477	0.60053	0.667255	0.66859	0.667922

During transient solution for melting process, mesh dependency was used to the current case study based on (PCM) average temperature PCM and liquid fraction. Figures 3.4 and 3.5 show the grid sizes studied to validate the numerical solution for grid size independence.

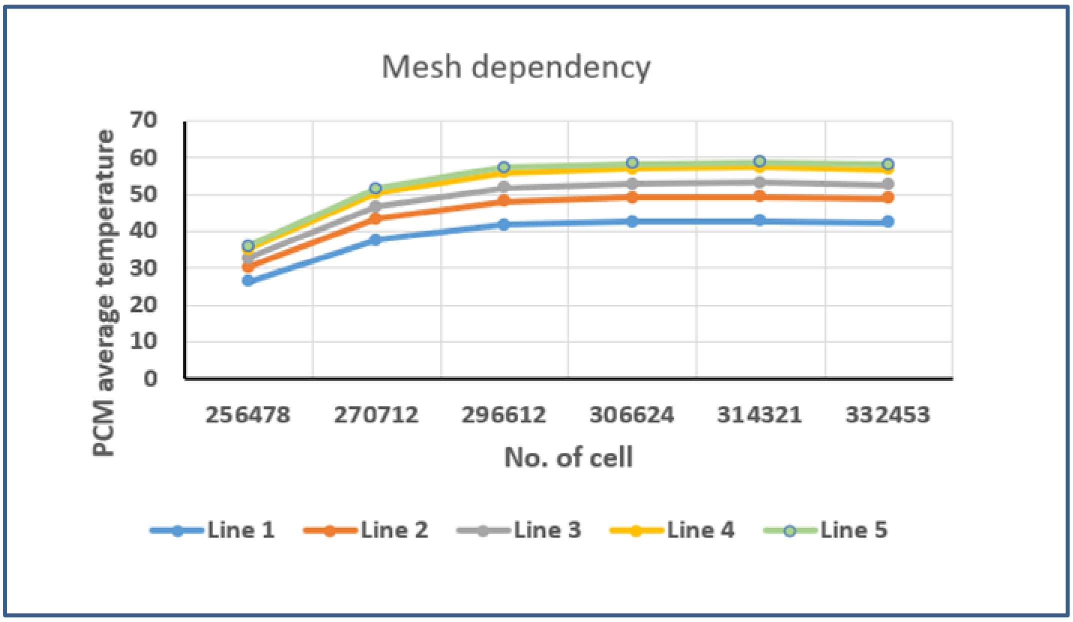

Figure 3.4: Mesh dependency tests for PCM average temperature.

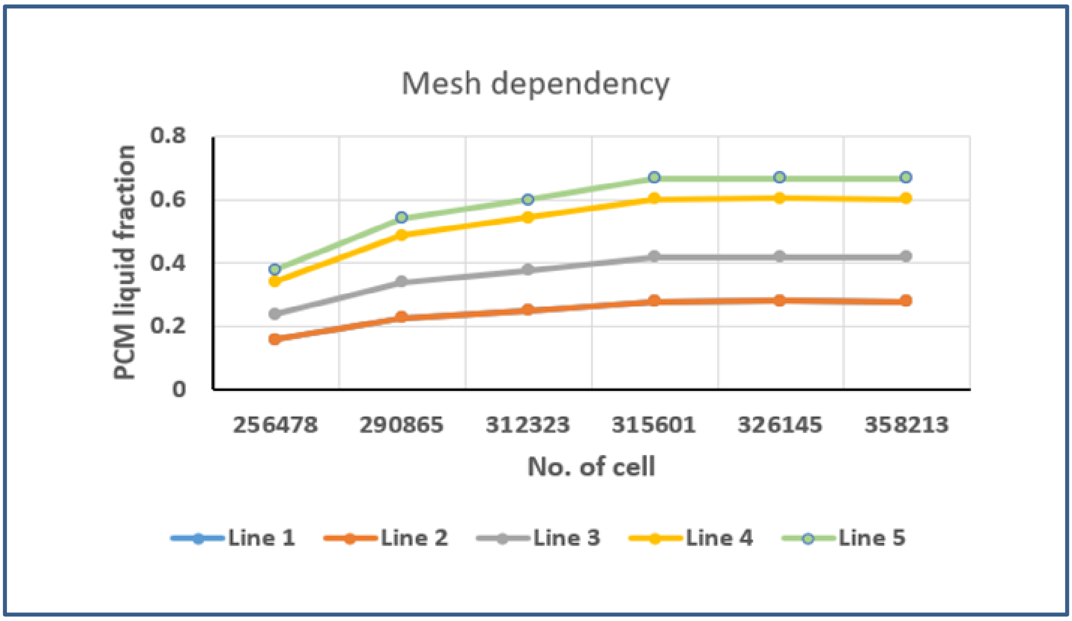

Figure 3.5: Mesh dependency tests for PCM liquid fraction.

3.8 Computational Grid

Grid generation or meshing is a very critical part of the CFD simulation process as it not only dictates the simulation time but also the accuracy of the results of the study. The mesh for the models is created using the mesh generation tool provided in the ANSYS-Fluent (workbench 2020 R2) program. The goal of making a mesh is to be able to input all of the domain geometry using high-quality cells. Therefore, when establishing the mesh, consideration must be given to the fact that it must be valid and conform to the domain boundary. Furthermore, the mesh density must be adjustable in order to achieve a balance between accuracy and solution time while also accounting for the amount of computer memory required for processing. There are different methods to obtain the computational grid, such as structured, unstructured and hybrid grid generation methods. Due to the complex geometry used in the current study, a structured grid generation method can be utilized to develop the computational mesh. This method, which relies on the quadrilateral shape is used to generate the computational grid of the present geometry. Figure 3.6 depicts the structure mesh that was employed in this study (315601). The time step is set to 0.01s and each time step has a number of 300. At each time step, with a convergence criterion of 10^{-6} for all variables. Half of the domain has been analyzed due of the symmetrical system around the concentric. This will significantly reduce the analysis time and improve the compatibility between the numerical simulation and the previous investigations, thereby reducing the error rate.

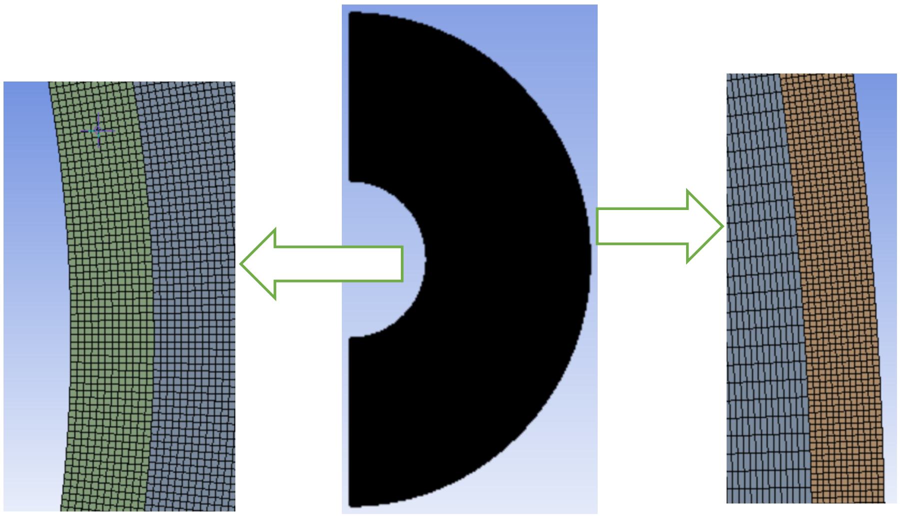

(A) (B) (C)

Figure 3.6: Mesh generation for the physical domain.

3.9 CFD Modeling and Simulation

Computational Fluid Dynamics (CFD) is the simulation of fluids engineering systems using modelling (mathematical physical problem formulation) and numerical methods (discretization methods, solvers, numerical parameters, and grid generations, etc). It is increasingly used to model the heat transfer and fluid flow in heat exchangers. A numerical simulation for each charging and discharging operations has been advanced effectively by using ANSYS-Fluent software (workbench 2020 R2). CFD shares with the numerical solution of differential equations governing the momentum, mass, and energy in the fluid problems. The mathematical formulation of the physical problem includes a set of partial differential equations, which are solved numerically by using finite volume method (FVM). Solving complex problems was the most challenging task in research laboratories and industry; therefore, using CFD analysis can solve this problem precisely. ANSYS Fluent software supplies the capability to modeling thermo-fluid problems, mesh them, apply the boundary conditions and simulating the status to get results.

CHAPTER FOURE

RESULTS AND DISCUSSION

4.1 Overview

In this chapter, the numerical simulation results have been presented for the melting and solidification processes of a PCM (paraffin wax) encapsulated between two concentric horizontal pipes. The results are discussed and explained in terms of temperature contours and liquid fraction distribution in the domain over a sixteen-hour time span. In addition, the grid independence test of the current numerical algorithm and the validation tests are displayed. On the other hand, it can be noted here that all results will be presented in the half-right domain only because the physical domain is symmetric about the θ-direction.

4.2 Validation Tests

In order to verify the CFD code in the present study, several comparisons were made with numerical published studies. The reliability of the simulation was validated by comparing the current numerical forecasts for the solidification process to prior findings of Al-Abidi et al [20] and Jasim et al [28] under the same conditions as shown in Figure 4.1. It can be observed that the predicted transient PCM temperatures are in good accordance with the other results. The validation results demonstrate that the current physical model and simulation are correct and dependable. In the physical configuration of the validation case study, the inner tube radius is 25.4 mm with 1.2 mm thickness, the middle tube radius is 75 mm and the outer tube radius is 100 mm with 2 mm thickness, all pipes are made from copper to ensure high thermal conductivity and to enhance heat transfer between the PCM and the heat transfer fluid [20].The minimum temperature required to operate the liquid desiccant air conditioning was approximately

65 °C. Water was used as fluid because of its high heat capacity and low cost, so the maximum charging temperature was 95 °C which equivalent to 13 °C temperature difference between the PCM and the heat transfer fluid. Finally, the validation case finds a good agreement the previous studies according the average error about 4.5% and 3.3% with [20] and [28] respectively.

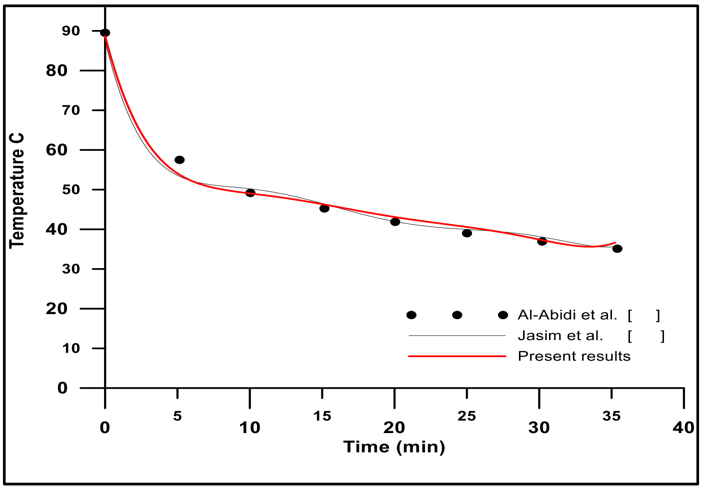

Figure 4.1: Comparison of temperature profile vs. previous studies Al-Abidi et al[20] and Jasim et al[28] .

Moreover, the accuracy of the finding was validated via the comparison of the current numerical forecasts for the melting process to prior results of Al-Abidi et al [20] and Al-Mudhafar et al [29] under the same conditions. Figure 4.2 presents the validation result. It can be observed that the predicted transient (PCM) temperatures are in good agreement with the other results. The validation results demonstrate that the current physical model and simulation are correct and dependable. In the physical configuration of the validation case study, all tubes are composed of copper to provide efficient thermal conductivity and to facilitate heat transmission between the (HTF) and the (PCM). The inner, middle, and outer tubes have a radius of 25.4 mm, 75 mm, and 100 mm, respectively. Also, the inner and outer tubes have a thickness of 1.2 mm and 2 mm, respectively [20]. More details about the validation case can be found in [20]. The maximum errors occurred between 8 minutes and 20 minutes during charging mode. Finally, the validation case finds good agreement with the previous studies, with an average error of about 3.7% and 2.9% with [20] and [29] respectively.

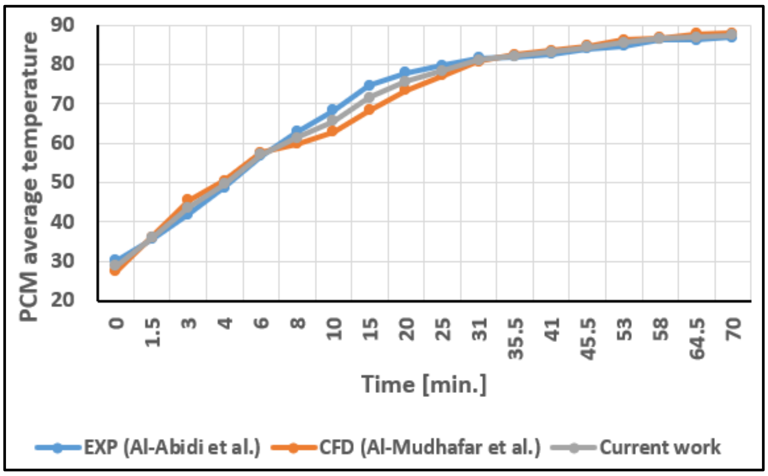

Figure 4.2: Comparison of the temperature profile with previous studies by Al-Abidi et al[20] and Al-Mudhafar et al[29].

4.3 Solidification Process

In order to evaluate the thermal performance of (PCM) in a horizontal shell-and-tube LHTES system during the solidification operation, low-temperature HTF is passed through the inner tube to remove thermal energy from the high-temperature liquid PCM in the annulus. The temperature of the PCM (67 °C) was higher than the melting point. Whereas, the cold HTF has a temperature of 27°C. Figure 4.3 presents the temperature contours of the PCM at different time steps from 0 s to 59575 s during the solidification process. At the initial time t = 0 s, the liquid fraction value is one, indicating that the state is liquid. Due to the hugely large temperature difference between liquid PCM and the HTF, the sensible heat of the PCM is removed by natural convection in the liquid PCM. As a result, the temperature of the PCM rapidly drops to the freezing point. When that happened, the PCM that surrounded the tube began to solidify, forming a solid PCM layer around the tube. It can be seen that the liquid of PCM decreases with the increasing thickness of the solid layer. The reason is that the thermal resistance increases with the increase in the thickness of the solid layer, leading to the heat exchange rate decreasing. Consequently, the decreased rate of heat transfer led to a decrease in the rate of PCM phase change from liquid to solid. This indicates that thermal conduction between the HTF and the solid/liquid interface controls the rate of solidification. The liquid fraction decreases gradually with time, convection circulation occurs in the liquid area of the PCM, causing a clockwise and anti-clockwise vortex to form to the left and right of the tube, respectively. The high-temperature liquid PCM flows upward due to natural convection, whereas the low-temperature liquid PCM flows downward due to gravity. On the other hand, effects of buoyancy and convective heat transfer can explain why the lower part of the PCM solidifies faster than the upper part. Thermal conduction dominates heat transport, giving adequate time for slow solidification. It takes approximately 16 hours for the PCM temperature to drop from 340 K to 302 K during a discharging process. The same behavior repeated in Figure 4.4 according to liquid fraction value. It is noted that the solid phenomena found on the bottom side of the annulus are due to the buoyancy force effect. Especially after 990 s until reaching a solid state after 5957 s.

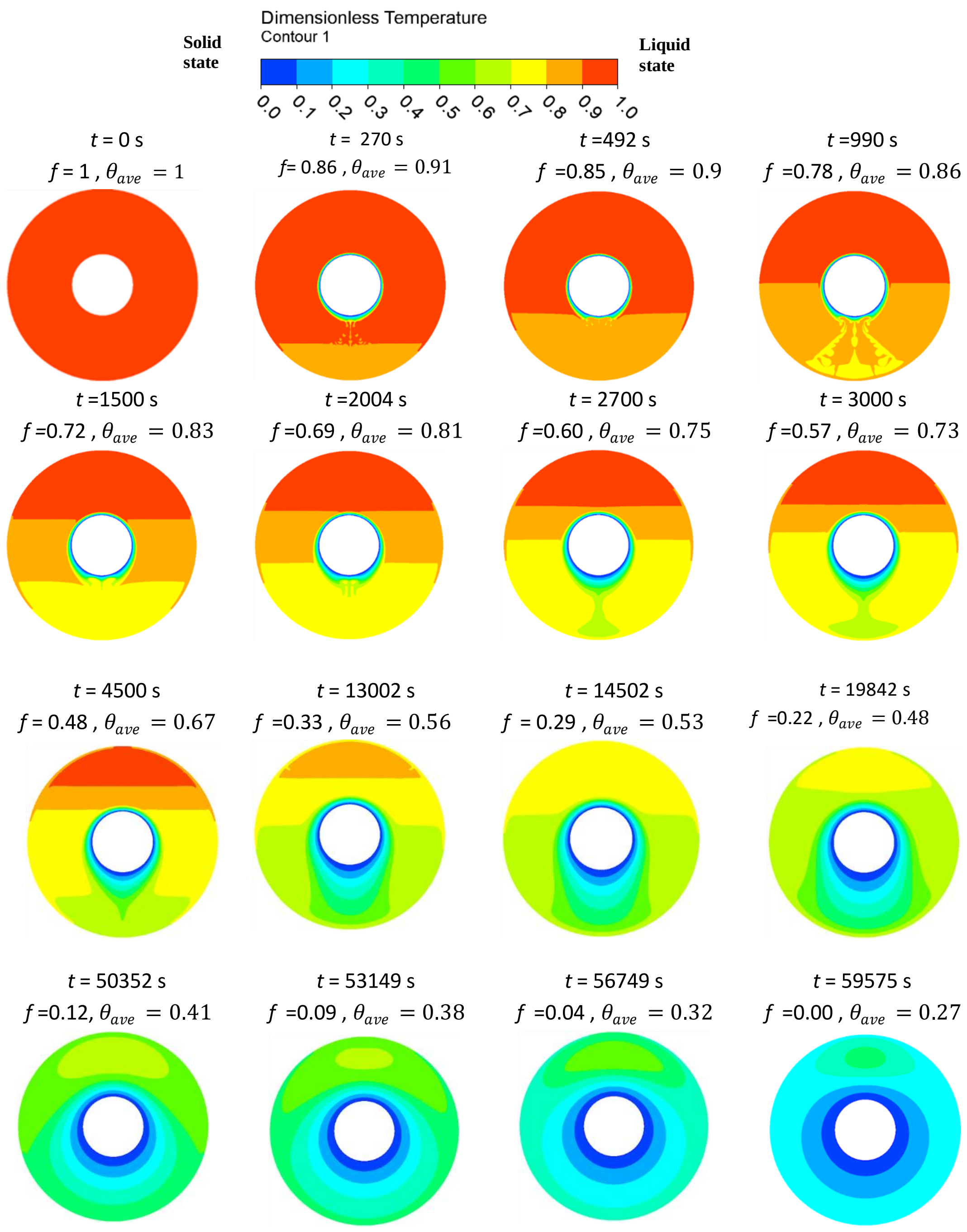

Figure 4.3: Contours of PCM transient temperature during discharging process.

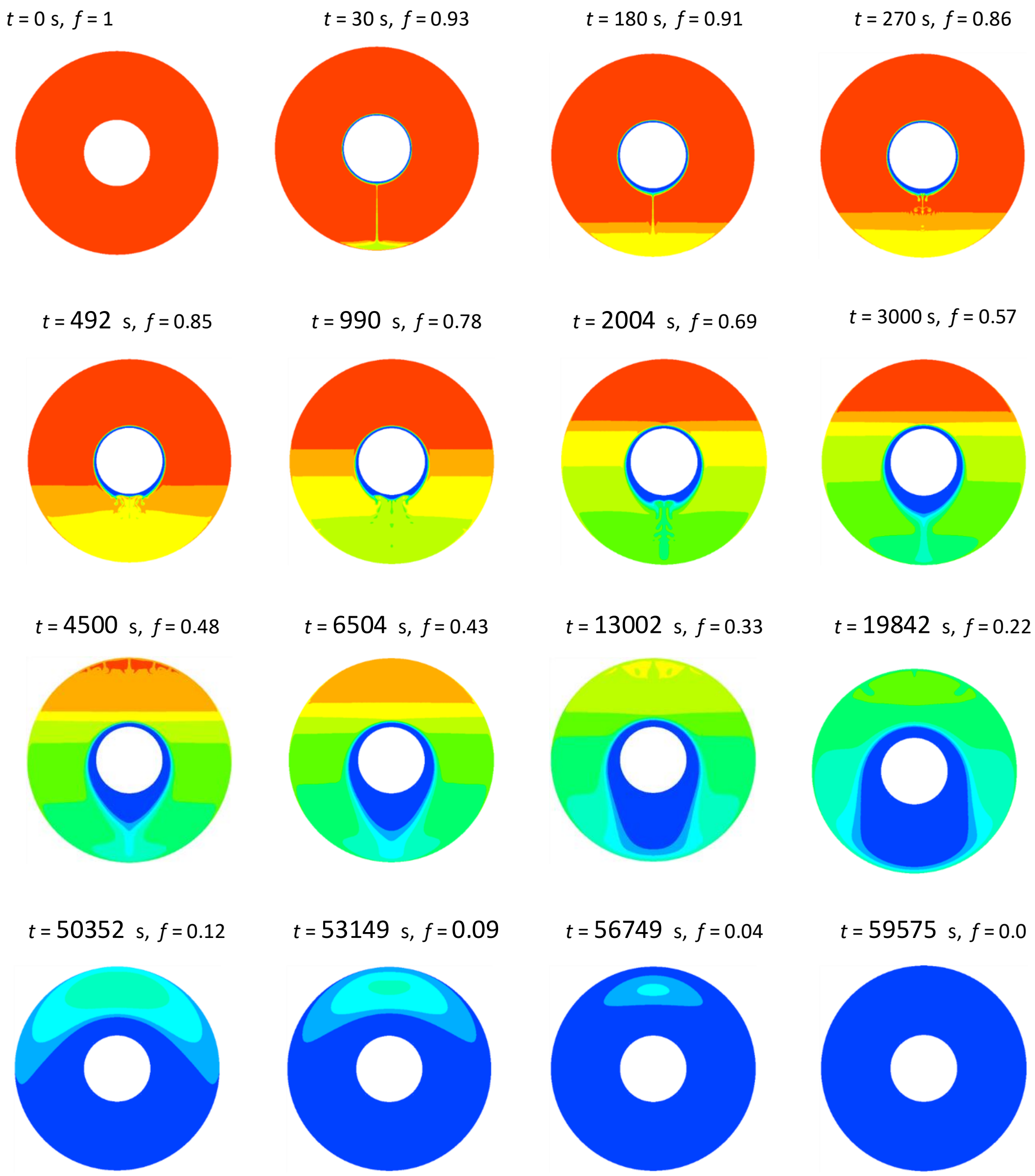

Figure 4.4: Contours of the PCM transient liquid fraction during discharging process.

Figure 4.5 shows the temperature distribution on the annulus radius in dimensionless form for different times and locations in the domain. Whereas at the beginning, the max. temperature did not exceed 55 ℃ at line 1, after that the time increase led to a decrease the temperature profile along line 1, where the solid state would dominate. But this distribution is irregular and depends on buoyancy force effects. Finally, after 16 hours, the maximum temperature reached 37℃. This drops in max. temperature along line 1 by 32% during this time period. The temperature gradient was small at the beginning, but it became strong as time increased, especially near the outer pipe surface. On the other hand, the temperature gradient is constant nearly from $\dot{R}R$=0.25 to the end of $\dot{R}R$=1 when time equals 3 hours (line 3), but after that the temperature gradient quickly becomes irregular due to solids phenomena. This behavior is repeated along other lines, but it is strong and quick.

$$RR= (R-R2)/(R3-R2)$$

It can be noted here that R_2 represents the outer radius of the inner tube, while R_3 represents the inner radius of the outer tube.

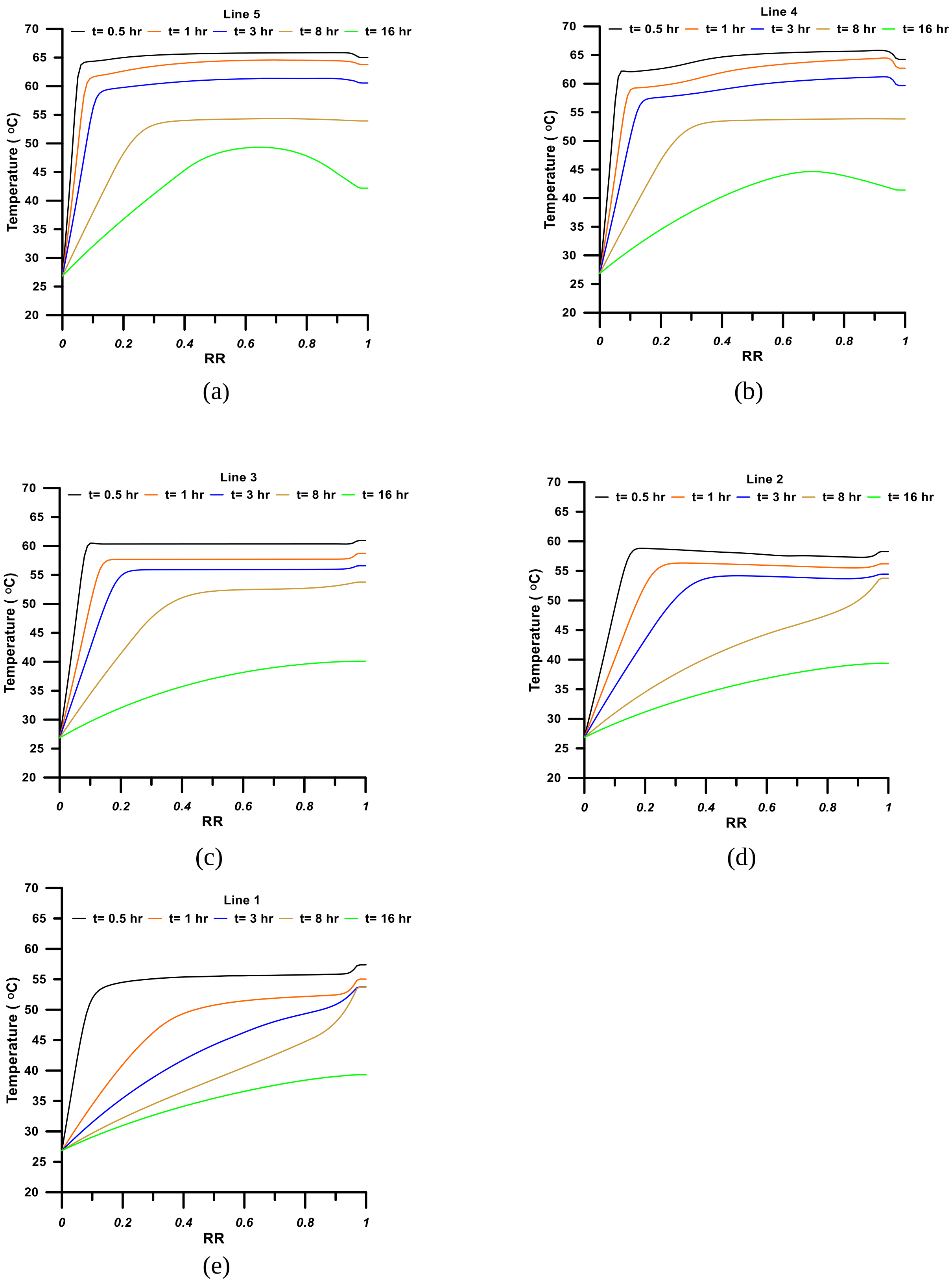

Figure 4.5: Temperature with dimensionless radius for different times and locations in the annulus:(a)Line5,(b)Line 4, (c) Line 3, (d) Line 2,(e) Line1.

Figure 4.6 presents the PCM transient liquid fraction contours during the discharging process, where the decrease from 1 at time=0 to 0 at time =59575 s. The temperature changes near the outer pipe surface during 16 hrs. can be seen in Table 4.1, while the liquid fraction changed during 16hrs as Table 4.2 according to Figures (4.5 & 4.6) as shown below. According to Table 4.1the temperature difference has lower value at line 1 while it is increase to higher value at line 5 due to line location in the dolman and bouncy force direction with or without gravity force. Table 4.2 presents the solid-state domain according to $\dot{R}R$ value in the annuls. Where $\dot{R}R$ near the zero leads that to the location near the inner tube surface where it is near to the HTF while when $\dot{R}R$ close to 1 that means neared to the outer tube surface. From the table the liquid fraction changes from lower value at starting time and it is increase gradually with time to reach 1 in the end of scarification processes approximately about 16 hr. In line 2 there is a fluctuation values of the liquid fraction values due to turbulence effects and bouncy force movement in this case.

Table 4.1: Temperature changes near the outer pipe surface during 16 hrs.

$\Delta T_{max.} = T_h - T_c$	$\Delta T = T - T_c$	Percentage = $\Delta T / \Delta T_{max.}$
Line 1	17 ℃	42.5 %
Line 2	18 ℃	45 %
Line 3	20 ℃	50 %
Line 4	21.8 ℃	54.5 %
Line 5	22.5 ℃	56.25 %

Table 4.2: Liquid fraction changes in the annulus during 16 hrs. according to $\dot{R}R$ value.

$\dot{R}R$ where $\dot{R}R = 0$ $at\ time = 0$					
Time (hr.)	0.5	1	3	8	16
Line 1	0.05	0.28	0.56	0.82	1
Line 2	0.025	0.14	0.23	0.68	0.98
Line 3	0.04	0.09	0.12	0.28	0.96
Line 4	0.025	0.05	0.08	0.18	0.94
Line 5	0.02	0.04	0.06	0.175	0.55

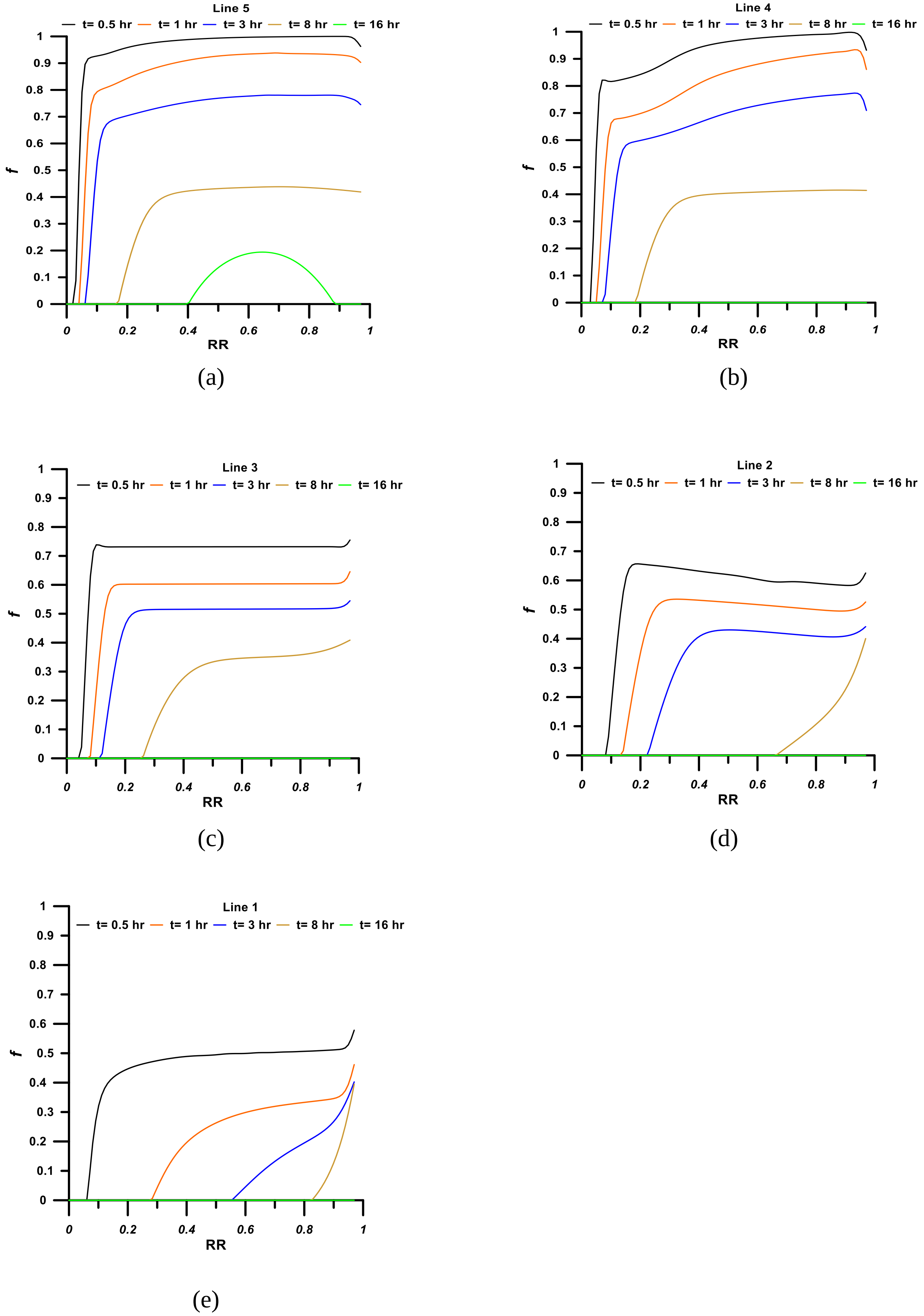

Figure 4.6: Liquid fraction with dimensionless radius for different times and locations in the annulus:(a)Line5,(b)Line4, (c)Line3,(d)Line2,(e)Line1.

4.4 Melting Process

To estimate the free convection in the melting operation, the average temperature and liquid fraction presented in graphical form as a function of time are displayed on the symmetric right-half separated by a vertical line passing through θ=0° and θ=180°. Figure 4.7 presents the history curves of the PCM average temperature over different line locations. It can be seen that conduction heat transfer leads to PCM melting in the vicinity of the inner pipe at first, but as the melt layer grows, convection heat transfer gradually takes control. Starting with the top line 5, which is located at the symmetry axis (θ=180°), (PCM) was solid at 27°C. The melting begins after an hour and a half to bring the PCM from its initial temperature to the melting point. It is evident that the PCM average temperature rises rapidly early on, which indicates that there is a high level of heat exchange between the cold (PCM) and the hot (HTF) surface via conduction heat transfer. Furthermore, it has been observed that over the course of five hours, the melting rate of PCM increases by more than 50%, while the average temperature rises to 59 °C. After this time, the curve becomes linear, and the average temperature stays consistent over all time spans (6hr, 10hr, and 11hr) at around 60°C, indicating a mushy phase transition operation in which the heat transfer rate between the PCM and the HTF is regulated by the integrated effect of convection and conduction via the phase change. Moreover, one can also find that this behavior is repeated along line 4 at an angle of 135°.It is evident that line 3 at position (θ=90°) has the same behavior as the preceding lines, with small differences. The mismatch in curve three occurs only at the start of the melting operation and at the end of that too. On the other hand, as demonstrated in this figure, the lines 2 and 1 at 45° and 0°, respectively, have similar trends and behave differently when compared to other lines. It can be observed that the global behavior of the curves varies with variation in position, i.e., the non-linearity of these curves increases as the angular degree deviates from 90° for all the line locations studied, as is illustrated in graph 4.8. Consequently, it's possible to draw the conclusion that the higher the evaluation line, the greater the temperature values are achieved for the entire simulation period. so that temperature changes are greatest at line5 (θ= 180°) and least at line1 (θ= 0°). This is owing to the buoyancy force discussed in the momentum equation (Equation (3.9)), which uses the Boussinesq approximation to account for density fluctuations with temperature, causing liquid (PCM) to have a specific velocity.

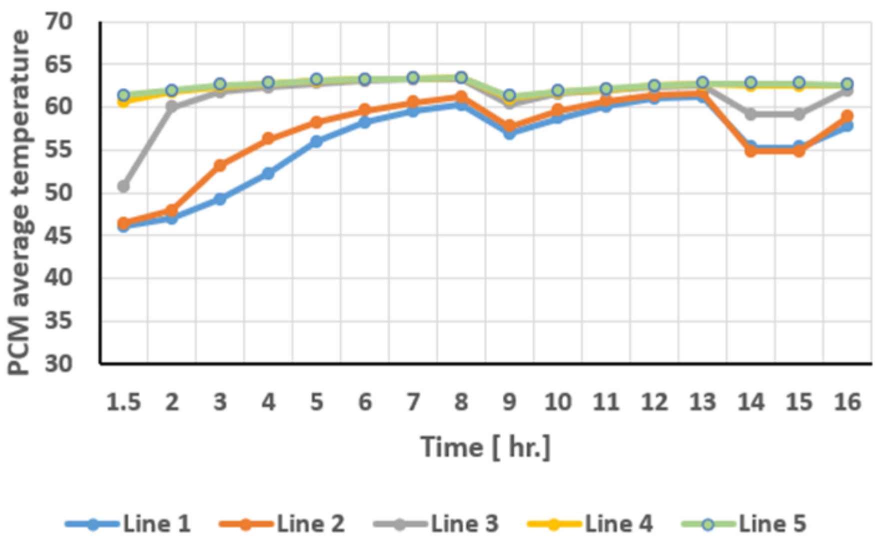

Figure 4.7: History of PCM average temperature over different line's locations during melting process.

To further confirm this conclusion, we additionally present the history of PCM liquid fraction for these five different line locations in the domain as shown in Figure 4.8. Based on the difference in the slopes of the locations of the lines, there are three stages to this operation. At the first stage, heat is mainly transferred through conduction. The liquid portion of PCM increases as time passes and the slop trend is sharp at first, then progressively weakens, indicating that the melting interface's thermal conductivity performance has been reduced. However, at this stage, the total liquid fraction value for variation locations at melting time, t = 1.5hrs, is 78 percent at line 5, 76 percent at line 4, 23 percent at line 3, and percent at lines 1 and 2. At the second stage, heat is transferred through conduction in the solid (PCM) and through the combined impact of conduction and free convection in the liquid (PCM). The total liquid fraction for this stage at melting time, t = 10, when compared to the corresponding values for the first stage, is 2% higher at line 5, 4% higher at line 4, 57% higher at line 3, 66% higher at line 2 and 60% higher at line 1. At the third stage, heat is transferred through both thermal natural convection and conduction. In this final stage of the charging cycle at t = 14hr, the total liquid fraction is 80% for the top region (lines 4 and 5), which in comparison to the middle region (line 3), is only 13% less, and in comparison, to the bottom region (lines 1 and 2), the liquid fraction is 38% lower. From the above quantitative findings, it is clear that the top zone of the annulus has a much higher melting rate than the bottom zone. As mentioned earlier, as confirmation of this, the melting process ends up with a relatively short period of time in the upper region, followed by the middle region, and eventually the lower region.

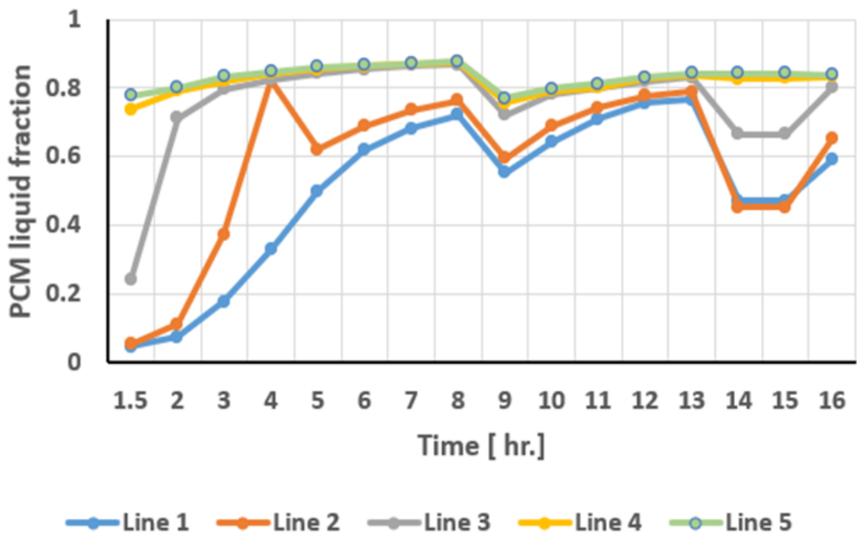

Figure 4.8: History of PCM liquid fraction over different lines locations during melting process.

Moreover, the temperature contours of the PCM are illustrated in Figure 4.9, including the liquidus (339K) and solidus (318.5K) temperatures. Between these two temperatures is the mushy zone. The concentrated temperature contours on the upper half of the inner tube surface suggest that this is where the greatest heat transmission occurs. The temperature contours during the melting process have a perfect cylindrical shape, showing that the major heat transport mechanism is conduction. Then it extends radially outwards. As charging time progresses, convection currents in the melt begin to move from the bottom part to the top part of the inner tube surface due to the movement of the fluid because of density variations arising from the heating effect, thereby implying that the charging process is being impacted by convection.

After that, the melt is forced to bend and flow downward along the relatively cool outer cylinder. At this point, the hot downward melt collides with a cooler solid. Because of the conduction and free convection, the downward motion of the melt is slowed by the resistance force supplied by the solid, and melting occurs on the top of the annulus in the radial and angular directions. With time elapsed, the hot melt moves down along the cold mushy region, subsequently losing energy, becoming colder, and eventually attaining the bottom of the solid region, meaning that convection has been replaced by conduction in the bottom zone. Moreover, the low thermal conductivity of the PCM decreases the conduction rate of heat transmission. Consequently, the melting rate in the lower zone of the annulus is much slower than in any other part of the annulus.

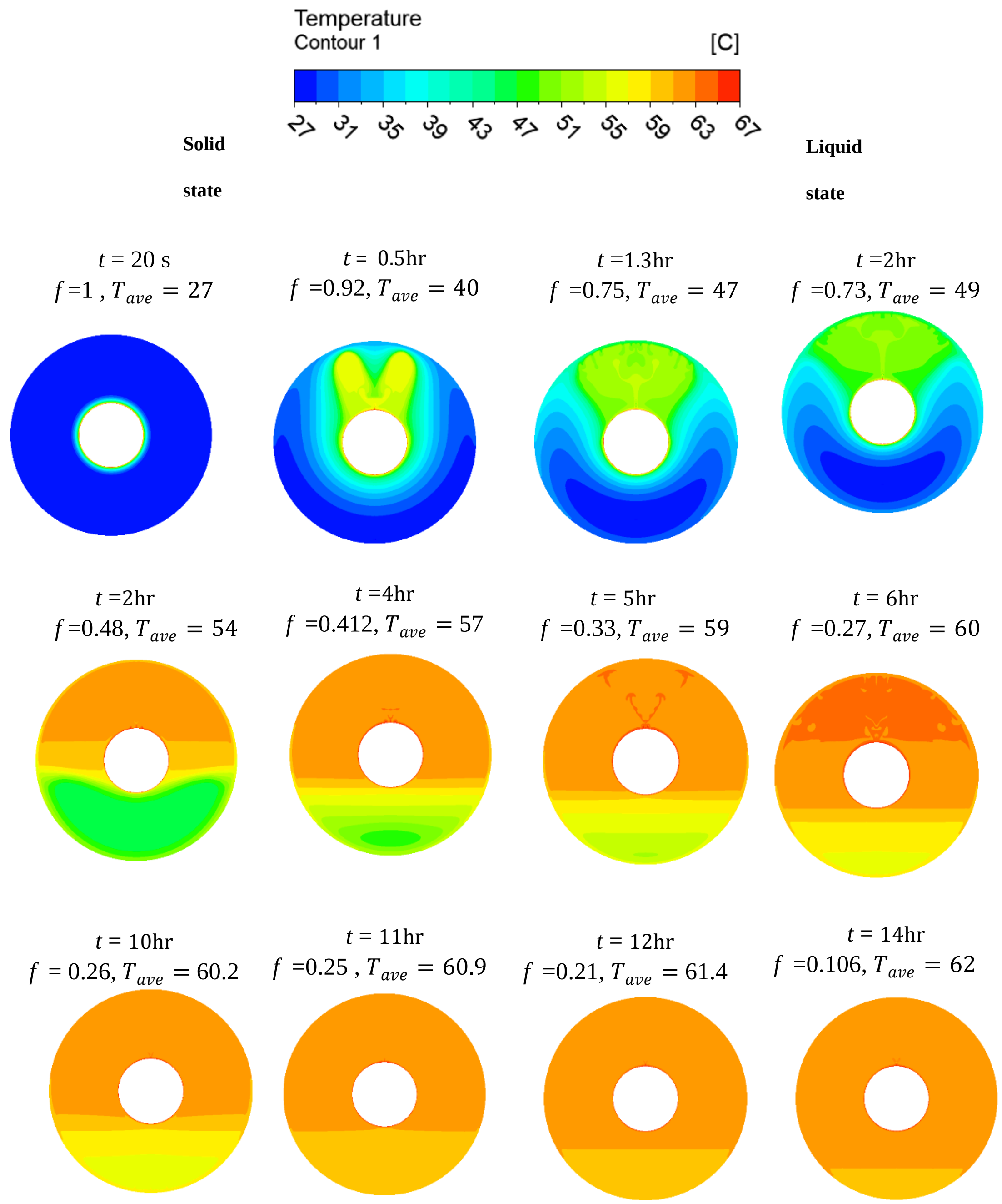

Figure 4.9: Contours of the PCM transient temperature during melting process.

Furthermore, to better understand the movement of the liquid-solid interface, the contours of the liquid fraction found in the numerical solution for the storage system are illustrated in Fig. 4.10. The liquid fraction (*f*) is measured using the following equation:

$$f = \frac{Volume\ of\ the\ liquid\ PCM}{Total\ volume\ of\ the\ PCM\ (solid+liquid)} \times 100$$

In the initial stage of melting, it can be seen that a very thin melting layer is formed around the inner tube at 20s. Because there is not enough liquid PCM to support natural convection and because convection has a limited influence on heat transfer, thermal conduction is the dominating heat transport mode. As a consequence, the trend of the solid-liquid interface is radially outwards. As time passes (t = 1.3hr), increasing the liquid fraction in melted PCM to 25% provides a bigger carrier for natural convection, resulting in the heat transmission mechanism being controlled by natural convection rather than conduction. With time, the melt gains heat and moves, carrying energy upward, driven by the buoyancy force. It then changes the flow direction under the influence of the temperature gradient when it reaches the top of the annulus and transfers energy to the vicinity of the liquid-solid interface. After 4 hours, the liquid fraction is up to 58%. Meanwhile, the phase change interface moves downward, the melting zone expands, and the liquid zone gradually thickens until it reaches the bottom region in a time span of 6 hours with an increasing liquid fraction of up to 73%. Furthermore, it is evident that in the final stage of the phase transition operation, the driving force of natural convection is reduced. Consequently, the PCM in the lower region will slowly melt. The reason why this phenomenon occurs is due to weaker buoyancy and increasing thermal resistance. Therefore, conduction plays a main role in the process of heat transmission at the bottom of the PCM. Figure 4.11 shows the history of local (PCM) temperature over different locations in the annulus. Generally, PCM local temperature decrees gradually with the line length due to the bouncy force direction effect as shown for lines 1, 3 and 5. Increasing the time value leads to converting the relationship from a curve to a line with a small change in PCM local temperature. The curves have a high temperature near the inner wall and then decrease with the direction of the outer wall. The same sequence is repeated in Figure 4.12, but according to the liquid fraction of PCM.

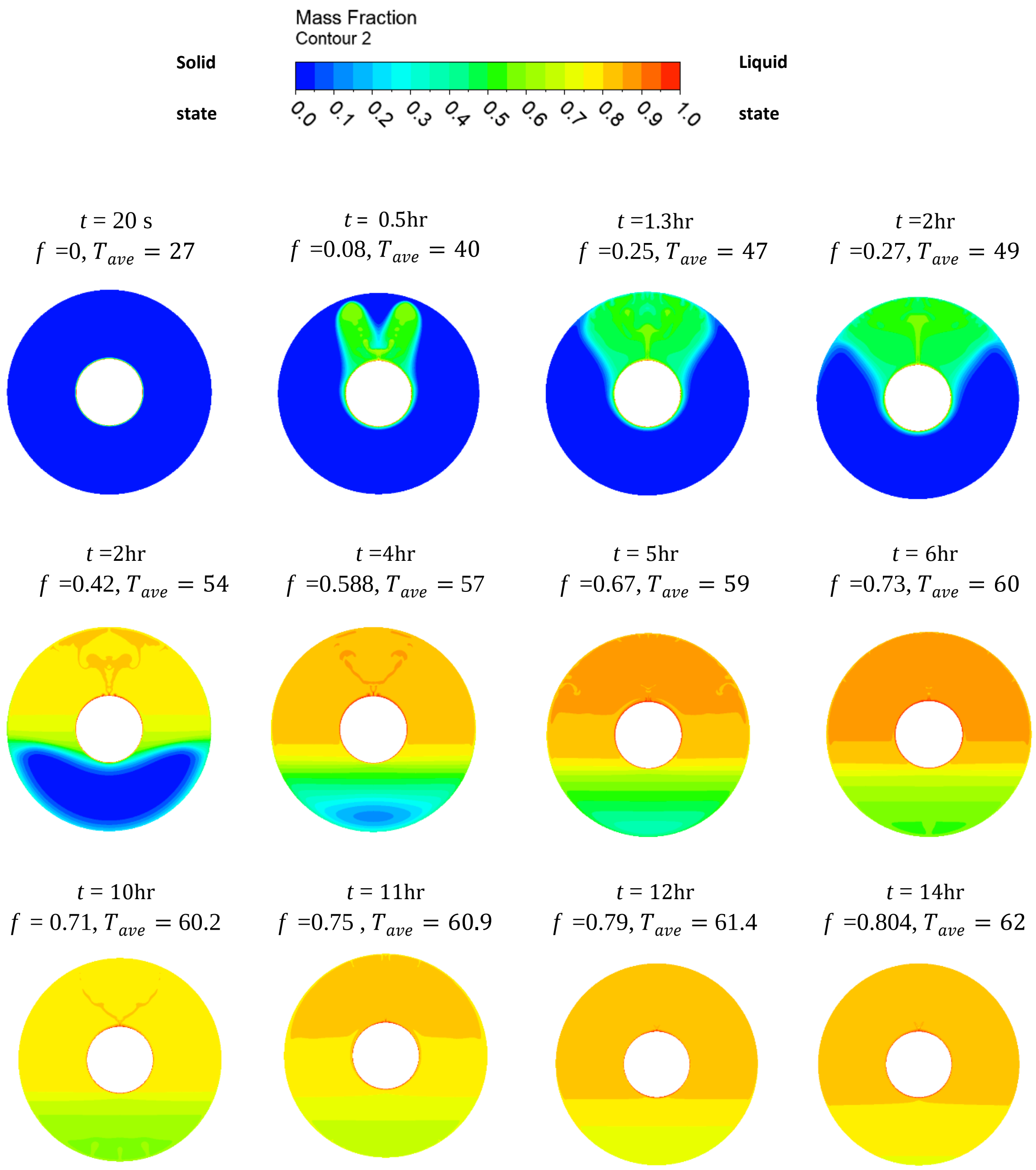

Figure 4.10: Contours of the PCM transient liquid fraction during melting process.

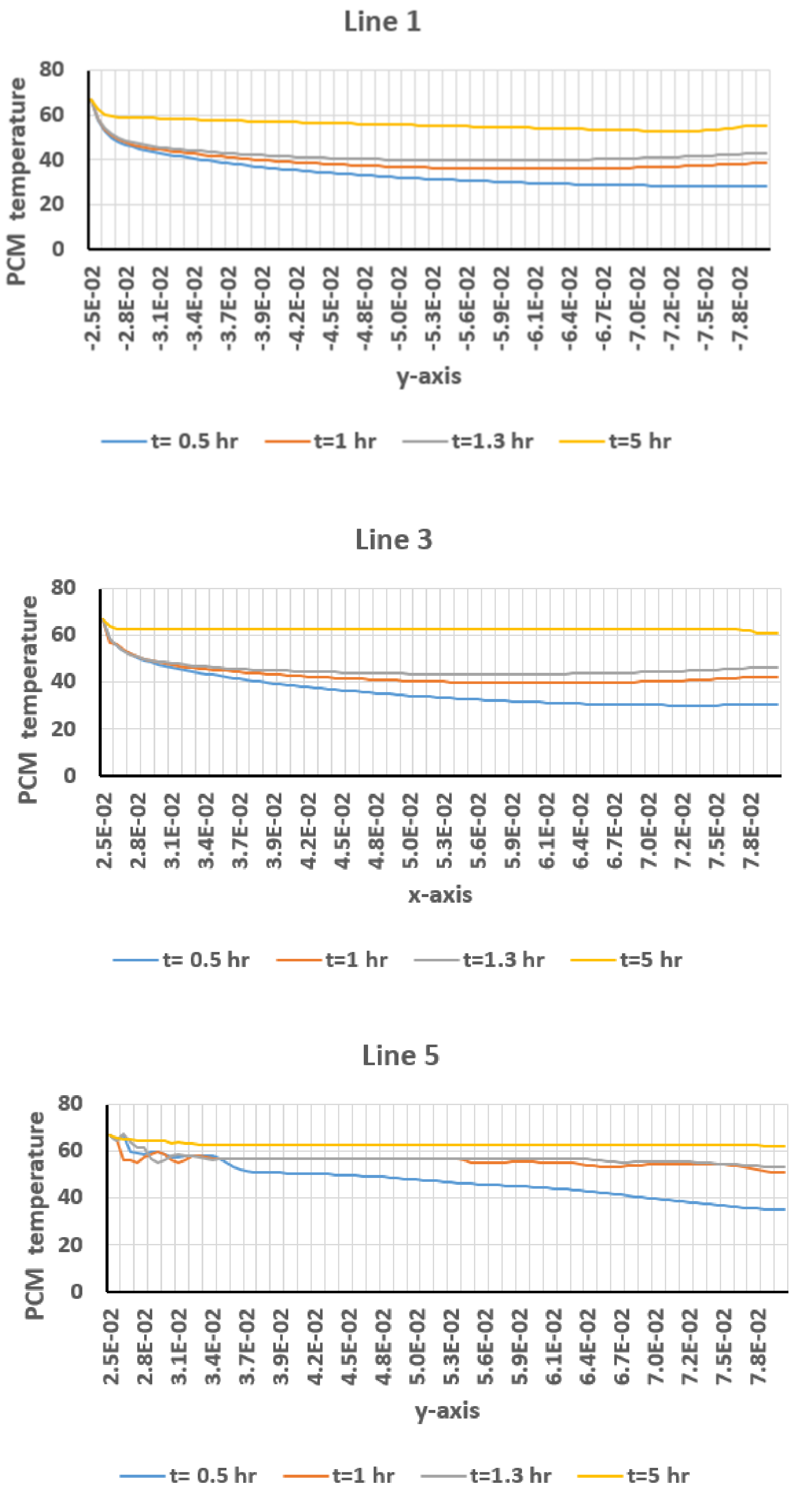

Figure 4.11: History of local PCM temperature over different line's locations.

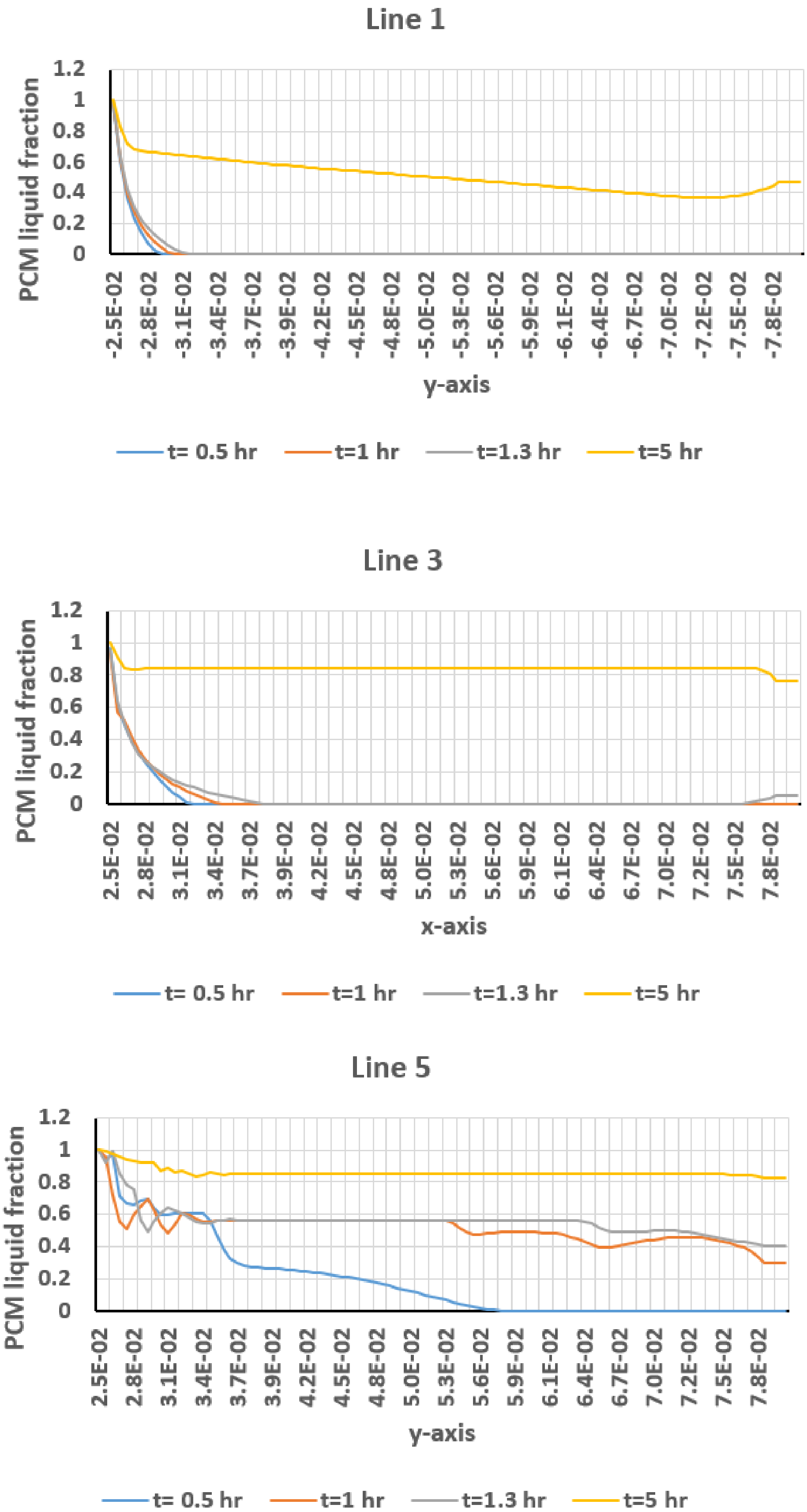

Figure 4.12: History of local PCM liquid fraction over different lines locations.

CHAPTER FIVE

Conclusion and Recommendations

5.1 Conclusion

In the precent study, an annulus model was established to predict the thermal energy storage specifications of a PCM (paraffin wax) when it is embedded in the annulus of a heat exchanger type double-pipe during melting operation. The model rests on solving the governing equations using the enthalpy-porosity method. An isothermal condition at the inner pipe surface and an adiabatic condition at the outer shell surface of the annulus have been considered. The numerical solution for the two-dimensional transition demonstrated conductive and complex conductive-convective heat transfer mechanisms in the solid, mushy zone, and molten phases, respectively.

During solidification process natural convection plays a significant role during its early periods. Thermal conduction remains the dominant heat transfer mode for the entire process. In the plain tube circumstance, the predicted result shows the capturing phenomenon: Heat conduction is the primary process in all regions, then heat convection and conduction become the dominant in the top and bottom regions, respectively. The maximum and minimum temperature changes near the outer pipe surface during 16 hrs. are 56.25 % and 42.5 % respectively. The findings of the visualization study are confirmed by the numerical results that show strong thermal stratification of the solidification process in the upper part of the tube.

According to the outcomes of the current computational investigation study of the combined buoyancy-driven and conduction melting of PCM, the following findings have been reached:

(1) The charging rate in the top part of the shell is faster as compared to the other regions, as buoyancy-driven convection is strengthened by the maximum growth of the melt zone.

(2) Only conduction occurs in the lowest half of the annulus during the later stages of the charging operation. As a result, the charging operation is extremely sluggish. The reason for this phenomenon is that the (PCM) employed in the current study has very poor heat conductivity.

(3) The charging process ends up with a relatively short period in the upper region, followed by the middle region, and finally the lower region of annulus. Consequently, the upper zone of (PCM) melts faster than the lower zone. The maximum and minimum temperature fluctuations nearer the pipe's outer surface during 16 hours are 43.75% and 31.25%, respectively.

5.2 Recommendations and Future work

According to the numerical results of the current study, the scope for future investigations can be listed as follows:

1. Experimental study can be proposed using the same parameters studied in the current research.
2. The current study can be extended to perform numerical solution in all three dimensions of the model.
3. Investigate the addition of nanoparticles to paraffin wax is a suggestion to improve the thermal conductivity.
4. The energy storage efficiency of the vertically oriented double-pipe LHTES system can be compared to that of the horizontally oriented LHTES system.
5. The study can be extended to investigate the effects of fins and extended surfaces on the thermal efficiency and thermal performance of the PCMs in general.
6. It may be beneficial to calculate the amount of heat flux in the processes of solidification and melting.

REFERENCES

[1] C. Suresh and R.P. Saini, "Review on solar thermal energy storage technologies and their geometrical configurations," *International Journal of Energy Research.*, vol. 44, no.6, pp.4163-4195, 2020.

[2] D.S. Mehta, K. Solanki, M.K. Rathod and J. Banerjee, "Thermal performance of shell and tube latent heat storage unit: Comparative assessment of horizontal and vertical orientation," *Journal of Energy Storage*., vol.23, pp.344-362, 2019.

[3] K. Du, J. Calautit, Z. Wang, Y. Wu and H. Liu, "A review of the applications of phase change materials in cooling, heating and power generation in different temperature ranges," *Applied energy*., vol. 220, pp.242-273,2018.

[4] F. Agyenim, N. Hewitt, P. Eames and M. Smyth, "A review of materials, heat transfer and phase change problem formulation for latent heat thermal energy storage systems (LHTESS)," *Renewable and sustainable energy reviews*., vol.14, no. 2, pp.615-628,2010.

[5] P.Bose and V.A. Amirtham, "A review on thermal conductivity enhancement of paraffin wax as latent heat energy storage material," *Renewable and Sustainable Energy Reviews*., vol. 65, pp.81-100,2016.

[6] M.H. Mahfuz, M.R. Anisur, M.A. Kibria, R. Saidur and I.H.S.C. Metselaar, "Performance investigation of thermal energy storage system with Phase Change Material (PCM) for solar water heating application," *International Communications in Heat and Mass Transfer*., vol. 57, pp.132-139, 2014.

[7] G.R. Dheep, and A. Sreekumar, "Influence of nanomaterials on properties of latent heat solar thermal energy storage materials-A review," *Energy conversion and management*., vol. 83, pp.133-148, 2014.

[8] A. Sharma, V.V. Tyagi, C.R. Chen and D. Buddhi, "Review on thermal energy storage with phase change materials and applications," *Renewable and Sustainable energy reviews*., vol.13, no.2, pp. 318-345,2009.

[9] R.M.R. Saeed, "Advancement in thermal energy storage using phase change materials," *Missouri University of Science and Technology*., 2018.

[10] S.D.Sharma, and K.Sagara, "Latent heat storage materials and systems: a review, "*International journal of green energy*., vol. 2, no.1, pp.1-56,2005.

[11] H. Nazir, M. Batool, F.J. B. Osorio, M. Isaza-Ruiz, X. Xu, K. Vignarooban, P. Phelan and A.M. Kannan, "Recent developments in phase change materials for energy storage applications: A review," International Journal of Heat and Mass Transfer., vol.129, pp.491-523,2019.

[12] I. Sarbu, and C. Sebarchievici , " A comprehensive review of thermal energy storage, " Sustainability., vol, 10, no.1, p.191, 2018.

[13] A.Abhat, D.Heine, M.Heinisch, N.A.Malatidis, and G.Neuer, "Development of a modular heat exchanger with integrated latent heat energy store, " *Final Report*.,1981.

[14] M.Akgün, O.Aydin, and K.Kaygusuz, "Experimental Study on Melting/Solidification Characteristics of a Paraffin as PCM,"Energy Conversion and Management., vol. 48 ,no.2,pp. 669–78,2007.

[15] M.K .Rathod, and J. Banerjee , "Experimental Investigations on Latent Heat Storage Unit Using Paraffin Wax as Phase Change Material," *Experimental Heat Transfer.,* vol. 27, no. 1,pp. 40–55, 2014

[16] S.P.Jesumathy, M. Udayakumar, S. Suresh, and S. Jegadheeswaran, "An Experimental Study on Heat Transfer Characteristics of Paraffin Wax in Horizontal Double Pipe Heat Latent Heat Storage Unit," *Journal of the Taiwan Institute of Chemical Engineers*.,vol. 45 ,no.4, pp. 1298–1306,2014.

[17]Shen, Gang, Xiaolin Wang, and Andrew Chan, "Experimental Investigation of Heat Transfer Characteristics in a Vertical Multi-Tube Latent Heat Thermal Energy Storage System," *Energy Procedia*.,vol. 160,PP.332–39,2019.

[18]N. Kousha, M. Rahimi, R. Pakrouh, and R. Bahrampoury, "Experimental Investigation of Phase Change in a Multitube Heat Exchanger," *Journal of Energy Storage*.,vol. 23 ,PP. 292–304 , 2019.

[19]W.W. Wang, K. Zhang, L. B. Wang, and Y. L. He, "Numerical Study of the Heat Charging and Discharging Characteristics of a Shell-and-Tube Phase Change Heat Storage Unit," *Applied Thermal Engineering* .,vol. 58,no. 1–2 ,PP. 542–53,2013.

[20]A.A.Al-Abidi, S.Mat, K.Sopian, M.Y.Sulaiman, and A.T.Mohammad, "Internal and external fin heat transfer enhancement technique for latent heat thermal energy storage in triplex tube heat exchangers, " *Applied thermal engineering*., vol.53,no.1, pp.147-156,2013.

[21]S.Seddegh, X. Wang, and A. D. Henderson, "Numerical Investigation of Heat Transfer Mechanism in a Vertical Shell and Tube Latent Heat Energy Storage System," *Applied Thermal Engineering*., vol.87,pp .698-706,2015.

[22]S.Seddegh, X. Wang, and A. D. Henderson, "A Comparative Study of Thermal Behaviour of a Horizontal and Vertical Shell-and-Tube Energy Storage Using Phase Change Materials," *Applied Thermal Engineering*., vol. 93, PP. 348–58 ,2016.

[23]M. Esapour, M. J. Hosseini, A. A. Ranjbar, Y. Pahamli, and R.Bahrampoury, "Phase Change in Multi-Tube Heat Exchangers." Renewable Energy., vol. 85, PP. 1017–25,2016.

[24]S.S.M. Ajarostaghi, M.A.Delavar, and A.Dolati, "Numerical Investigation of Melting Process in Horizontal Shell-and-Tube Phase Change Material Storage Considering Different HTF Channel Geometries." *Heat Transfer Research*., vol.48, no.16,pp.1515–19,2017.

[25]G.S.Han, , H.S. Ding, Y. Huang, L.G. Tong, and Y.L.Ding, "A comparative study on the performances of different shell-and-tube type latent heat thermal energy storage units including the effects of natural convection, " International Communications in Heat and Mass Transfer,vol. 88, pp.228-235,2017.

[26]A. Elmeriah, D. Nehari, and M. Aichouni, "Thermo-Convective Study of a Shell and Tube Thermal Energy Storage Unit," *Periodica Polytechnica Mechanical Engineering*.,vol. 62 ,no.2,PP.101–9, 2018.

[27]L. Begum, M. Hasan, and G.H. Vatistas ,"Energy Storage in a Complex Heat Storage Unit Using Commercial Grade Phase Change Materials: Effect of Convective Heat Transfer Boundary Conditions," *Applied Thermal Engineering.*,vol. 131,PP. 621–41, 2018.

[28]J.M. Mahdi, and E.C. Nsofor, "Solidification enhancement of PCM in a triplex-tube thermal energy storage system with nanoparticles and fins , "*Applied Energy*.,vol. 211, pp.975-986,2018.

[29]A.H.Al-Mudhafar, A.F.Nowakowski, and F.C.Nicolleau, " Thermal performance enhancement of energy storage systems via phase change materials utilising an innovative webbed tube heat exchanger, " *Energy Procedia*., vol.151, pp.57-61,2018.

[30]M.S.Mahdi, H. B. Mahood, A. F. Hasan, A.A. Khadom, and A. N. Campbell, "Numerical Study on the Effect of the Location of the Phase Change Material in a Concentric Double Pipe Latent Heat Thermal Energy Storage Unit," Thermal Science and Engineering Progress .,vol.11,PP. 40–49,2019.

[31]L. Kalapala,, and J. K. Devanuri,"Parametric investigation to assess the melt fraction and melting time for a latent heat storage material based vertical shell and tube heat exchanger," Solar Energy .,vol.193 ,pp. 360-371,2019.

[32]A.N.A. Ghafoor, and M.A. Mussa, "Numerical Study of A Thermal Energy Storage System With Different Shapes Inner Tubes"., vol.15,no.4,PP. 21-35, 2020.

[33]M. K. Soni, N. Tamar, and S. Bhattacharyya, "Numerical simulation and parametric analysis of latent heat thermal energy storage system," Journal of Thermal Analysis and Calorimetry., vol. 141, no. 6, pp. 2511-2526,2020.

[34]G. Shen, X.Wang, A.Chan, F. Cao, and X. Yin, "Investigation on optimal shell-to-tube radius ratio of a vertical shell-and-tube latent heat energy storage system, "*Solar Energy*., vol. 211, pp.732-743,2020.

[35]Jian-you, Long, "Numerical and Experimental Investigation for Heat Transfer in Triplex Concentric Tube with Phase Change Material for Thermal Energy Storage," *Solar Energy*.,vol. 82 no.11,PP. 977–85,2008.

[36]M.J. Hosseini, , A. A. Ranjbar, K. Sedighi, and M. Rahimi, "A Combined Experimental and Computational Study on the Melting Behavior of a Medium Temperature Phase Change Storage Material inside Shell and Tube Heat Exchanger," International Communications in Heat and Mass Transfer.,vol. 39,n0.9,PP. 1416–24, 2012.

[37]Longeon, Martin, Adèle Soupart, Jean François Fourmigué, Arnaud Bruch, and Philippe Marty, "Experimental and Numerical Study of Annular PCM Storage in the Presence of Natural Convection," Applied Energy., vol.112,PP.175–84, 2013.

[38]M. A.Kibria , M. R. Anisur, M. H. Mahfuz, R. Saidur, and I. H.S.C.Metselaar, “Numerical and Experimental Investigation of Heat Transfer in a Shell and Tube Thermal Energy Storage System”,International Communications in Heat and Mass Transfer.,vol. 53,PP. 71–78,2014.

[39]M. J. Hosseini, M. Rahimi, and R. Bahrampoury, “ Experimental and Computational Evolution of a Shell and Tube Heat Exchanger as a PCM Thermal Storage System,” International Communications in Heat and Mass Transfer.,vol. 50,PP.128–36,2014.

[40]N. Kousha, M. J. Hosseini, M. R. Aligoodarz, R. Pakrouh, and RBahrampoury, “Effect of Inclination Angle on thePerformance of a Shell and Tube Heat Storage Unit – An Experimental Study.” Applied Thermal Engineering.,vol. 112,PP. 1497–1509,2017.

[41]S.Seddegh, M.M. Joybari, X.Wang, and F. Haghighat,“Experimental and Numerical Characterization of Natural Convection in a Vertical Shell-and-Tube Latent Thermal Energy Storage System,” Sustainable Cities and Society.,vol. 35,PP.13–24,2017.

[42]A.D. Korawan, S. Soeparman, W. Wijayanti, and D.Widhiyanuriyawan, “3D Numerical and Experimental Study on Paraffin Wax Melting in Thermal Storage for the Nozzle-and-Shell,Tube-and-Shell, and Reducer-and-Shell Models,” Modelling and Simulation in Engineering., 2017.

[43]I.Al Siyabi, , S. Khanna, T.Mallick, and S.Sundaram, “An Experimental and Numerical Study on the Effect of Inclination Angle of Phase Change Materials Thermal Energy Storage System,” Journal of Energy Storage .,vol.23 ,PP. 57–68, 2019.

[44]R.B.Mahani, H.I. Mohammed, J.M. Mahdi, F.Alamshahi, M.Ghalambaz, P.Talebizadehsardari and W.Yaïci, “ Phase change process in a zigzag plate latent heat storage system during melting and solidification, ” *Molecules*., vol.25, no.20, p.4643,2020.

[45]A.D.Brent, V.R. Voller, and K.T.J. Reid. “Enthalpy-porosity technique for modeling convection-diffusion phase change: application to the melting of a pure metal,” *Numerical Heat Transfer, Part A Applications*., vol. 13, pp.297-318 ,1988.

[46]P.Talebizadeh Sardari, G.S.Walker, M.Gillott, D.Grant, and D.Giddings, “Numerical modelling of phase change material melting process embedded

in porous media: Effect of heat storage size, ” *Proceedings of the institution of mechanical engineers, Part A: journal of power and energy*., vol. pp.234, 365-383 ,2020.

[47]A.A.Al-Abidi, S.B.Mat, K. Sopian, M. Y. Sulaiman, and A.T.Mohammed. “CFD applications for latent heat thermal energy storage: a review,” *Renewable and sustainable energy reviews*., vol. 20, pp.353-363, 2013.

[48]H.M.Ali, “Applications of combined/hybrid use of heat pipe and phase change materials in energy storage and cooling systems: a recent review, ” *Journal of Energy Storage*., vol. 26, pp.100986,2019.

[49] R.B.Mahani, H.I. Mohammed, J.M. Mahdi, F.Alamshahi, M.Ghalambaz, P.Talebizadehsardari, and W.Yaïci, “Phase change process in a zigzag plate latent heat storage system during melting and solidification, ” *Molecules*.,vol. 25,pp. 4643 ,2020.

[50]M.M.Joybari, F.Haghighat, and S.Seddegh, “Numerical investigation of a triplex tube heat exchanger with phase change material: Simultaneous charging and discharging, ” *Energy and buildings*.,vol. 139, pp.426-438 ,2017.

[51]R. Ahmadi, M.J. Hosseini, A.A. Ranjbar, R. Bahrampoury,“ Phase change in spiral coil heat storage systems,”Sustainable cities and society.,vol.38, P.145-57,2018.

[52]A.j. Parry, P.C. Eames, F.B. Agyenim,“Modelling of thermal energy storage shell-and-tube heat exchanger,” Heat Transfer Engineering, vol. 35,no.1, pp. 1-4, 2014.

الخلاصة

تم إجراء دراسة عددية ثنائية الأبعاد، تهدف إلى فهم دور الحمل الحراري لقوة الطفو أثناء ذوبان وتصلب مواد تغيير الطور (PCMs) داخل مبادل حراري مزدوج الأنبوب وفقًا للمقطع العرضي للحلقة. تم اختيار شمع البرافين المحلي على أنه مادة متغيرة الطور بدرجة حرارة انصهار تبلغ 334 كلفن. تم اختيار الماء على أنه سائل نقل الحرارة (الماء الساخن للشحن والماء البارد للتفريغ) يتدفق عبر الأنبوب الداخلي. الظروف الحرارية لسطح الانبوب الخارجي معزول (كاظم الحرارة) وسطح الانبوب الداخلي ثابت عند درجة حرارة معينة (ثابت الحرارة). تم استخدام طريقة الحجوم المحددة(FVM) لحل المعادلات الحاكمة لحالة غير المستقرة لجريان طباقي المطوَّر بالكامل. تم حساب تدفق السوائل في المنطقة الطرية باستخدام مصطلح مصدر سحب دارسي في الزخم، وتم تحديث النسبة المئوية للسائل في كل خلية باستخدام طريقة المحتوى الحراري– المسامية.

بينت النتائج العددية بأن انتقال الحرارة بالحمل الحراري له تأثير كبير على ذوبان المنطقة العليا من شمع البرافين ولكن تأثيره أقل على ذوبان المنطقة السفلية. من الواضح أن عملية الذوبان تنتهي بفترة زمنية قصيرة نسبيًا في المنطقة العليا، تليها المنطقة الوسطى، وأخيراً المنطقة السفلية من الحلقة. وكذلك وجد أن الحد الأقصى والأدنى لتغيرات درجة الحرارة بالقرب من سطح الأنبوب الخارجي خلال 16 ساعة هي 43.75 بالمائة و31.25 بالمائة على التوالي.

أثناء عملية التصلب، نقل الحرارة بالحمل الحراري له دور مهم خلال الفترات المبكرة من التصلب بينما يهيمن التوصيل على نقل الحرارة للعملية بأكملها. توضح النتيجة المتوقعة ظاهرة الالتقاط: يصبح التوصيل الحراري الأولي في جميع المناطق ثم الحمل الحراري والتوصيل سائدًا في المناطق العلوية والسفلية، على التوالي. الحد الأقصى والأدنى لتغيرات درجة الحرارة بالقرب من سطح الأنبوب الخارجي خلال 16 ساعة هي 56.25 بالمائة و42.5 بالمائة على التوالي.

جمهوريـــــــــة العـــــــــراق
وزارة التعليم العالي والبحث العلمي
جامــعــة الانبار – كـلـيـة الهـنـدسة
قســـم الهندســـة الميكانيكيـــــة

دراسة مادة متغيرة الطور تستخدم في أنظمة الطاقة الشمسية لتخزين الطاقة الحرارية

رسالة مقدمة إلى مجلس
كـلـيـة الهـنـدسة ـ جامــعــة الانبـار
وهي جزء من متطلبات نيل درجة الماجستير
في علوم الهندسة الميكانيكية

أعداد

بلقيس عبد عباس الفهداوي
(بكالوريوس هندسة ميكانيكية – 2018)

باشراف
أ.م.د. مصطفى برزان عبد الغفور

1443هـ 2022م